Journal of Building Engineering 104 (2025) 112317

Contents lists available at ScienceDirect

Journal of Building Engineering

journal homepage: www.elsevier.com/locate/jobe

Full length article

Weather-adaptive fuzzy control of setpoints for energy-efficient HVAC in urban buildings

Mojtaba Safdari [a], Mohammad Al Janaideh [a], Kamran Siddiqui [b], Amir A. Aliabadi [a,*]

[a] School of Engineering, University of Guelph, Guelph, Ontario, Canada
[b] Department of Mechanical and Materials Engineering, Western University, London, Ontario, Canada

ARTICLE INFO

Dataset link: http://www.aaa-scientists.com/, https://github.com/AmirAAliabadi

Keywords:
Building energy modeling
Fuzzy Logic Controller
Sensible and latent loads
Smart building
Weather-adaptive control

ABSTRACT

This paper presents a novel Weather-Adaptive Fuzzy Control (WAFC) strategy to dynamically manage indoor temperature and humidity setpoints for improved energy efficiency in urban buildings. The main contribution lies in integrating external weather data, electricity prices, and occupancy levels within a fuzzy control framework to continuously align indoor setpoints with varying outdoor conditions. The WAFC utilizes external weather conditions, electricity prices, and occupancy levels to adapt the setpoints of a building's Heating, Ventilation, and Air Conditioning (HVAC) system. A key innovation of this approach is the adaptive alignment of indoor conditions with outdoor temperatures and humidity levels, allowing the HVAC system to adjust to changing environmental conditions effectively. The Fuzzy Logic Controller (FLC) calculates a control variable (w) to determine optimal setpoints, balancing energy use with occupant comfort. The WAFC is compared to a traditional fixed setpoint strategy, with results indicating that the WAFC significantly reduces heating and humidification demands, particularly in high Air Changes per Hour (ACH) conditions. Although cooling and dehumidification demands are increased under smart control during the summer, the total annual energy savings achieved by WAFC was 274 kW-hr m^{-2} for a typical detached residential house in Toronto, demonstrating its potential for enhancing energy efficiency. Sensitivity analyses demonstrate that WAFC effectively reduces energy consumption for diverse building types, particularly for older, less airtight buildings. The findings suggest that weather-adaptive setpoint control can significantly enhance the sustainability of HVAC operations, providing a practical solution for energy efficiency in urban environments.

1. Introduction

According to a 2023 report by the International Energy Agency (IEA), in 2022, buildings accounted for 30% of global final energy consumption, a significant share of the total energy consumption across various sectors, with space heating and cooling representing the largest energy consumption end uses in the building sector. As the global energy demand reached 440 EJ, energy consumption in buildings rose by an average of 1.1% per year from 2010 to 2022. In cold climates, space heating is the dominant energy use in buildings, with floor area projected to expand from 157 billion m^2 in 2022 to 170 billion m^2 by 2030. Meanwhile, space cooling is seeing the fastest growth, fueled by rising incomes, especially in developing economies, and the increasing intensity of heat waves.

* Corresponding author.
E-mail addresses: msafdari@uoguelph.ca (M. Safdari), aaliabad@uoguelph.ca (A.A. Aliabadi).
URL: https://www.aaa-scientists.com (A.A. Aliabadi).

https://doi.org/10.1016/j.jobe.2025.112317
Received 13 December 2024; Received in revised form 5 February 2025; Accepted 6 March 2025
Available online 15 March 2025

Despite significant efficiency improvements, space cooling remains a growing source of energy demand due to the rapid adoption of air conditioners [1].

In addition, electrification plays a critical role in reducing the environmental impact of heating and cooling in buildings. Heat pumps, for instance, are emerging as a more energy-efficient alternative to gas boilers, using three to five times less energy. In 2022, heat pumps met 12% of global space heating demand, and this share is expected to more than double to 25% by 2030 in the IEA's Net Zero Emissions (NZE) scenario. The increasing adoption of these technologies, combined with improvements in energy efficiency, is essential for reducing both energy consumption and emissions in the building sector. While challenging power grids, the shift to renewable energy sources, particularly electricity from renewable sources, is expected to offer consumers greater control and flexibility through demand response systems, helping to align with global sustainability goals [2].

As these trends highlight the importance of energy-efficient technologies in managing building energy use, the focus on effectively controlling Heating, Ventilation, and Air Conditioning (HVAC) systems becomes even more critical [3]. HVAC systems are not only responsible for significant energy consumption but also play a key role in maintaining a comfortable and healthy indoor environment. To achieve this balance, optimizing the performance of these systems is essential, particularly in terms of how they regulate indoor climate conditions [4]. Among various factors such as temperature, humidity, lighting, and air quality, that influence Indoor Environmental Quality (IEQ) [5] and thermal comfort [6–8], temperature and humidity are the most critical parameters. Proper control of these variables ensures a comfortable indoor climate and prevents damage to building and HVAC equipment by adjusting HVAC operations according to occupancy and external conditions [9,10]. Setpoint control is a fundamental aspect of HVAC system operation. It involves establishing desired values for temperature and humidity, which the control system strives to maintain. By optimizing setpoints, building operators can reduce energy consumption without compromising indoor conditions [11].

A variety of methods have been employed to regulate the desired temperature or humidity within a space, a process commonly referred to as setpoint control. Traditional approaches to setpoint control often involve the use of continuously operating thermostats that maintain a fixed temperature or humidity [12,13]. Unfortunately, this method may prove inadequate in adapting to fluctuating conditions or dynamic occupancy patterns. Another common strategy is to utilize programmable thermostats or humidistat that adhere to pre-determined schedules created by building occupants. While this approach offers some flexibility, it also presents drawbacks. Occupants may be reluctant to invest the time and effort required to meticulously program and adjust thermostats or humidistats [14]. Additionally, there is often a discrepancy between planned occupancy schedules and actual usage patterns, which can lead to unnecessary heating or cooling and increased energy consumption. Research studies have yielded inconsistent results regarding the impact of constant or programmable setpoints on energy savings, with some investigations demonstrating positive effects and others revealing negative consequences. Recent advancements in sensor technology and the Internet of Things (IoT) have facilitated the development of thermostats and humidistats equipped with reactive controllers. These controllers possess the ability to dynamically adjust setpoints in real time based on changes in occupancy levels. However, a delay inevitably occurs between the detection of increased occupancy and the HVAC system's response, prompting the emergence of predictive controller systems.

Over the years, various control strategies have been developed to manage energy consumption in buildings, each with its advantages and limitations. Among the most commonly used methods are On/Off [15], Proportional-Integral-Derivative (PID) control [16], Model Predictive Control (MPC) [17–19], Fuzzy Logic Control (FLC) [20–22], as well as hybrid approaches that combine these techniques [23,24].

Proportional-Integral-Derivative (PID) and On/Off Controls are among the oldest and most widely used control strategies in HVAC systems due to their simplicity, ease of implementation, and low initial cost [25]. On/Off Control can be either zero (Off) or maximum (On), which makes it less accurate [15]. PID controllers work by adjusting control outputs based on the error between a desired setpoint and the actual system output, using a combination of proportional, integral, and derivative actions. While effective for linear systems, PID control struggles with the nonlinearities, time delays, and uncertainties often present in Building Energy Management Systems (BEMS). Additionally, PID controllers require extensive tuning and calibration, limiting their adaptability to changing conditions for instance the tuning process for Multi Input and Multi Output (MIMO) processes is sometimes impossible [26]. These limitations can lead to suboptimal performance in complex BEMS applications [27]. Model Predictive Control (MPC) offers a more sophisticated approach by predicting future system behavior based on a dynamic model and optimizing control actions accordingly. MPC is particularly well-suited for complex, multi-variable systems where interactions between variables and constraints need to be managed [28]. However, the implementation of MPC in BEMS is challenged by its high computational demands and the need for an accurate system model, which can be difficult to obtain in real-world settings [15,29]. FLC provides an alternative by mimicking human decision-making processes [30,31]. Unlike traditional controllers, FLC does not rely on precise mathematical models but instead uses a set of fuzzy rules to handle the inherent uncertainties and nonlinearities in BEMS [32]. This makes FLC particularly effective in maintaining thermal comfort in dynamic environments, where conditions may change unpredictably [33]. Moreover, hybrid control strategies, such as Fuzzy-PID and Neural Network-based MPC (NN-MPC), have been developed to combine the strengths of these individual methods. Fuzzy-PID control, for instance, enhances the adaptability of traditional PID controllers by using FLC to adjust the control parameters in real-time, improving performance in systems with varying dynamics [34]. NN-MPC integrates neural networks within the MPC framework to approximate complex system models, offering a more flexible and robust control solution [35]. FLC's ability to handle uncertainties, adapt to changing conditions, and operate without requiring a precise mathematical model makes it particularly well-suited for the dynamic and complex nature of BEMS [36,37]. A recent study further extended FLC by integrating it with Long Short-Term Memory (LSTM) networks, achieving improved predictive control for variable stiffness structures under seismic excitations [22].

Recently, Barte et al. [38] developed an automatic temperature and humidity control system for a tarantula terrarium using an FLC algorithm. This system ensures the maintenance of optimal environmental conditions, which are crucial for the health of

invertebrates like tarantulas. By utilizing FLC to control devices such as heat lamps, fans, and water pumps, the system was able to regulate temperature and humidity with minimal error, outperforming manual methods. The success of this system highlights the potential of FLC in managing sensitive environmental parameters.

In another recent study, Shao et al. [39] proposed a Weights-Based Fuzzy Logic Control Algorithm (WBFLCA) to enhance temperature and humidity control in direct expansion air-conditioning systems. The approach simplifies FLC by using weighted control rules, enabling decoupled and efficient management of both parameters. The study identified optimal weight combinations that improve system response and control stability, showcasing the potential for energy-efficient climate control in buildings.

The literature on humidity control is notably less extensive than that on temperature control. Some studies, such as Zhang et al. [40], have examined humidity control but omitted key factors relevant to human comfort. Their approach, which includes monitoring CO_2 concentration, temperature, condensation risk, and Relative Humidity (RH), uses dehumidifier and natural ventilation; however, humidity is the last criterion considered, with a maximum threshold of 88%, a notably high level that far exceeds ASHRAE 62.1 recommendations [41], where 65% is the advised upper limit for comfort and safety. Moreover, Zhang et al. [40] primarily focus on hot and humid conditions and regions, with minimal attention to year-round control or other climate zones. The high threshold for humidity also indicates a lack of focus on condensation and mold growth risks, as an RH of 88% could increase susceptibility to these issues.

To the best of our knowledge, most existing controllers and smart building research [42] focus on systems that adjust indoor setpoints based on sensor data, particularly occupancy detection [43]. These smart building systems typically adapt setpoints based on the presence or absence of occupants or use zone-based HVAC control to optimize comfort in specific areas. The intelligence of these HVAC systems is largely limited to detecting changes in occupancy level and responding accordingly, often ignoring other influential environmental factors [44]. However, the concept of a physically intelligent building, one that is environmentally aware and adapts indoor setpoints based not only on occupancy but also on real-time outdoor conditions, electricity pricing, and latent heat loads, remains underexplored in the current literature. Such an approach, integrating both internal and external factors, has the potential to significantly improve energy efficiency and overall comfort, addressing gaps that conventional smart building technologies have yet to address.

Furthermore, conventional temperature and humidity control strategies in HVAC systems typically rely on maintaining indoor conditions at fixed comfort setpoints or setbacks, often based solely on occupancy detection. This static approach neglects opportunities to leverage favorable outdoor conditions, even when they align well with indoor comfort requirements, leading to suboptimal energy performance. Such systems fail to capitalize on naturally occurring temperature and humidity levels that could otherwise be utilized to reduce HVAC loads, resulting in unnecessary energy consumption and inefficiency.

In this study, we introduce a novel Weather-Adaptive Fuzzy Control (WAFC) strategy that dynamically adjusts indoor temperature and humidity setpoints based on real-time data, including outdoor conditions, occupancy levels, and electricity prices. This approach moves beyond traditional static setpoints by incorporating a more comprehensive understanding of building's internal and external environment, providing a holistic optimization of HVAC performance. Unlike conventional systems, WAFC adapts continuously, not only during peak occupancy periods but also during energy-saving modes, allowing the indoor environment to converge with the outdoor climate whenever it is beneficial. This adaptive alignment reduces energy use while maintaining acceptable comfort levels, effectively utilizing natural opportunities for efficiency gains.

Moreover, WAFC addresses several key gaps in traditional control approaches. It considers both sensible and latent loads comprehensively, ensuring that humidity and temperature control are integrated in a way that optimizes both energy efficiency and occupant comfort. This represents a significant advancement in HVAC setpoint decision-making, integrating external environmental data to enable an environmentally-aware and physically intelligent building.

The remainder of this paper is structured as follows. In Section 2, the methodology is outlined, including a detailed description of the model and the proposed Weather-Adaptive Fuzzy Control (WAFC) strategy. Section 3 presents the results and discussion, where we analyze the performance of the WAFC and provide insights into its effects on energy efficiency, considering both sensible and latent loads. Finally, Section 4 concludes the paper with a summary of findings and offers recommendations for future research.

2. Methodology

2.1. Model description

Urban physics is simulated in this study by employing the Vertical City Weather Generator (VCWG v3.0.0) software (Fig. 1). VCWG is a multi-physics, micro-scale model that predicts urban climate and building performance by parameterizing key physical processes. VCWG integrates system-level models to simulate momentum, heat, humidity, and water exchanges across soil, urban surfaces, and the atmosphere, with options for including alternative energy systems. VCWG integrates models using the Resistance Capacitance (RC) thermal network, Navier–Stokes transport modeling in the vertical direction, Monin-Obukhov Similarity Theory (MOST), and bulk energy modeling paradigms [45]. As shown in Fig. 1, VCWG consists of several sub-models, including rural MOST model, urban vertical transport model, radiation model, building energy model, and rural/urban soil and surface energy balance models. Full descriptions of the model are provided in earlier publications [46–51]. The weather boundary conditions for VCWG are generated using another software titled the Vatic Weather File Generator (VWFG v1.0.0), which uses the ERA5 dataset from the European Centre for Medium-Range Weather Forecasts (ECMWF). VWFG provides data in the EnergyPlus Weather (EPW) file format at hourly resolution that is required by VCWG. The forcing weather files are associated with a rural site in the vicinity of each city [52]. The VCWG's results for a base building have been validated against observations of gas and electricity consumption

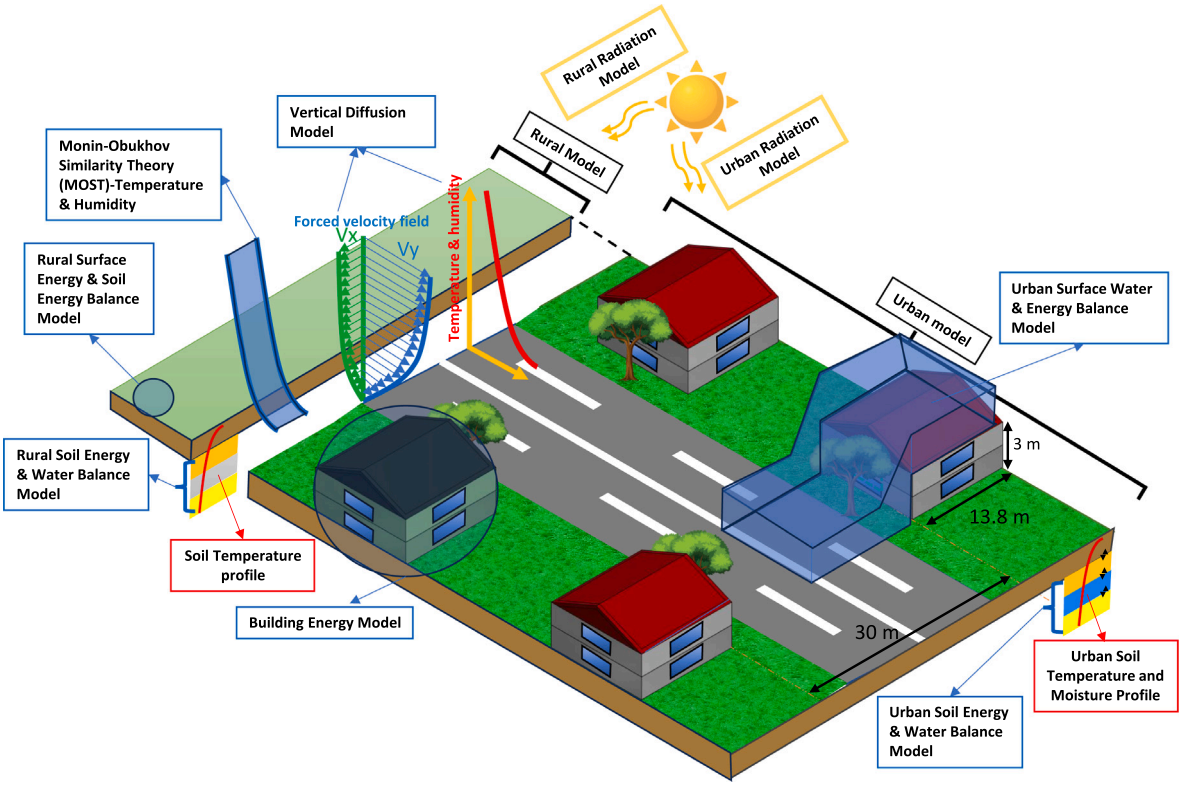

Fig. 1. Illustration of the Vertical City Weather Generator (VCWG v3.0.0) model and the constituent sub-models.

Table 1
Building features for Climate Zones (CZ) 5 from codes and standards.

Parameter	Toronto (CZ5)
Roof resistance [m^2 K W^{-1}]	6.41
Wall resistance [m^2 K W^{-1}]	3.6
Window U-value [W m^{-2} K^{-1}]	1.9
Infiltration rate [ACH]	3.0
Ventilation rate [L s^{-1} m^{-2}]	0.3
Glazing ratio [–]	0.4
Solar heat gain coefficient [–]	0.4

in London, Ontario, Canada, for a full year in 2019 [53]. This paper extends the model by integrating a Fuzzy Logic Controller (FLC). The model is developed and run for Toronto for the full year of 2020.

Fig. 1 shows the arrangement of single detached residential buildings considered in this study. Such houses are prevalent in North America and account for 52.6% and 64% of residential building stock in Canada [54] and the United States [55], respectively. The building features for each city are based on common codes and standards such as the National Energy Code of Canada for Buildings (NECB) [56], the American Society of Heating, Refrigerating and Air-Conditioning Engineers (ASHRAE) 62.1 [41], ASHRAE 62.2 [57], ASHRAE 90.1 [58], and ASHRAE 90.2 [59]. Table 1 shows the code and standard values for the base building features that we have used in our study.

The buildings are arranged in rows with a separation of 30 m maintained in each horizontal direction (x and y). Temperature, specific humidity, and wind (the x and y components) data within the urban roughness sub-layer were extracted along the vertical direction (z) from VCWG. The buildings are low-rise residential units designed with dimensions of 13.8 m × 13.8 m × 6 m. Each storey features two windows on each side, with an equivalent area of 26.4 m^2 per facade.

2.2. Building energy and environmental loads

The sensible load of the building, involves ventilation load Q_{vent}, infiltration load Q_{inf}, internal heat from occupants and equipment Q_{int}, heat from the building's mass Q_{mass}, heat from walls Q_{wall}, heat from ceilings Q_{ceil}, heat conduction through windows Q_{win}, and radiant heat passing through windows Q_{tran} [W],

$$\text{Sensible Load} = \pm \left[Q_{vent} + Q_{inf} + Q_{int} + Q_{mass} + Q_{wall} + Q_{ceil} + Q_{win} + Q_{tran} \right]. \quad (1)$$

In this formulation, the positive sign (+) will be used to calculate the sensible cooling demand, and the negative sign (−) will be used to calculate the sensible heating demand. Except for Q_{int}, which is scheduled in VCWG, the other terms are parameterized using the heat balance method:

$$\begin{aligned} Q_{\text{vent}} &= V_{\text{vent}}\rho_a c_{pa}(T_{\text{outdoor}} - T_{\text{set}}) \\ Q_{\text{inf}} &= V_{\text{inf}}\rho_a c_{pa}(T_{\text{outdoor}} - T_{\text{set}}) \\ Q_{\text{mass}} &= A_{\text{bui}} h_m (T_{\text{mass}} - T_{\text{set}}) \\ Q_{\text{wall}} &= A_{\text{wall}} h_w (T_{\text{wall}} - T_{\text{set}}) \\ Q_{\text{ceil}} &= A_{\text{bui}} h_c (T_{\text{ceil}} - T_{\text{set}}) \\ Q_{\text{win}} &= A_{\text{win}} U_w (T_{\text{outdoor}} - T_{\text{set}}) \\ Q_{\text{tran}} &= A_{\text{win}} S \times SHGC, \end{aligned} \tag{2}$$

where V_{vent} and V_{inf} [$m^3\ s^{-1}$] are ventilation and infiltration air flow rates, ρ_a [$kg\ m^{-3}$] is density of air, c_{pa} [$J\ kg^{-1}\ °C^{-1}$] is heat capacity of air, T_{mass}, T_{wall}, T_{ceil}, T_{set}, and T_{outdoor} [°C] are mass, wall, ceiling, set-point, and outdoor temperatures, A_{bui}, A_{wall}, and A_{win} [m^2] are building footprint, wall, and window areas, h_m, h_w, and h_c [$W\ m^{-2}\ °C^{-1}$] are convective heat transfer coefficients, U_w [$W\ m^{-2}\ °C^{-1}$] is the window U-value, S [$W\ m^{-2}$] is the shortwave radiation flux through the window, and $SHGC$ [-] is Solar Heat Gain Coefficient for the window, which is a constant. $SHGC$ [-] is based on code and standard values. However, a detailed two-dimensional radiation balance model predicts the shortwave and longwave radiation fluxes on each building surface (including the wall). The radiation model also predicts incident angles for these fluxes as well as shading effects from trees and other buildings. This model utilizes view factors and a Monte-Carlo ray tracing methodology [47]. However, incident angle effects on $SHGC$ [-] are not considered. This approach simplifies the modeling process, while it does account for dynamic variations of radiative fluxes due to weather, solar position, or shading. Future work could explore adaptive $SHGC$ [-] values to improve accuracy. These loads are met by the building's sensible cooling/heating equipment. The latent load,

$$\text{Latent Load} = \pm \left[Q_{\text{latvent}} + Q_{\text{latinf}} + Q_{\text{latint}} \right], \tag{3}$$

involves latent heat from ventilation Q_{latvent}, latent heat from infiltration Q_{latinf}, and latent heat from internal heat from occupants and equipment Q_{latint} [W]. In this formulation, the positive sign (+) will be used to calculate the dehumidification demand, and the negative sign (−) will be used to calculate the humidification demand. These loads are met by the building's humidification/dehumidification equipment. Except for Q_{latint}, which is scheduled in VCWG as a fraction of sensible heat from occupants and equipment Q_{int}, the other terms are parameterized using the humidity balance method:

$$\begin{aligned} Q_{\text{latvent}} &= V_{\text{vent}}\rho_a L_v (q_{\text{outdoor}} - q_{\text{set}}) \\ Q_{\text{latinf}} &= V_{\text{inf}}\rho_a L_v (q_{\text{outdoor}} - q_{\text{set}}), \end{aligned}$$

where L_v [$J\ kg_v^{-1}$] is latent heat of vaporization for water, and q_{outdoor} and q_{set} [$kg_v\ kg^{-1}$] are outdoor and set-point specific humidities, respectively.

Following the sign conventions discussed above, the heat balance equation can be rewritten in the following form, which separates terms including or excluding the unknown indoor temperature

$$\underbrace{\text{Cooling Load} - \text{Heating Load} - Q_{\text{tran}} - Q_{\text{int}}}_{Q} = Q_{\text{vent}} + Q_{\text{inf}} + Q_{\text{mass}} + Q_{\text{wall}} + Q_{\text{ceil}} + Q_{\text{win}} \tag{4}$$

$$\begin{aligned} Q = &\underbrace{V_{\text{vent}}\rho_a c_{pa} T_{\text{outdoor}} + V_{\text{inf}}\rho_a c_{pa} T_{\text{outdoor}} + A_{\text{bui}} h_m T_{\text{mass}} + A_{\text{wall}} h_w T_{\text{wall}} + A_{\text{bui}} h_c T_{\text{ceil}} + A_{\text{win}} U_w T_{\text{outdoor}}}_{H1} \\ &- [\underbrace{V_{\text{vent}}\rho_a c_{pa} + V_{\text{inf}}\rho_a c_{pa} + A_{\text{bui}} h_m + A_{\text{wall}} h_w + A_{\text{bui}} h_c + A_{\text{win}} U_w}_{H2}] T_{\text{indoor}}. \end{aligned} \tag{5}$$

Likewise the specific humidity balance equation can be rewritten as the following form, which separates terms including or excluding the unknown indoor specific humidity

$$\underbrace{\text{Dehumidification Load} - \text{Humidification Load} - Q_{\text{latint}}}_{QL} = Q_{\text{latvent}} + Q_{\text{latinf}} \tag{6}$$

$$QL = \underbrace{V_{\text{vent}}\rho_a L_v q_{\text{outdoor}} + V_{\text{inf}}\rho_a L_v q_{\text{outdoor}}}_{HL1} - [\underbrace{V_{\text{vent}}\rho_a L_v + V_{\text{inf}}\rho_a L_v}_{HL2}] q_{\text{indoor}}. \tag{7}$$

In VCWG v3.0.0, the resulting two equations $T_{\text{indoor}} = (H1 - Q)/H2$ and $q_{\text{indoor}} = (HL1 - QL)/HL2$ are re-evaluated in each timestep to give the indoor temperature and specific humidity.

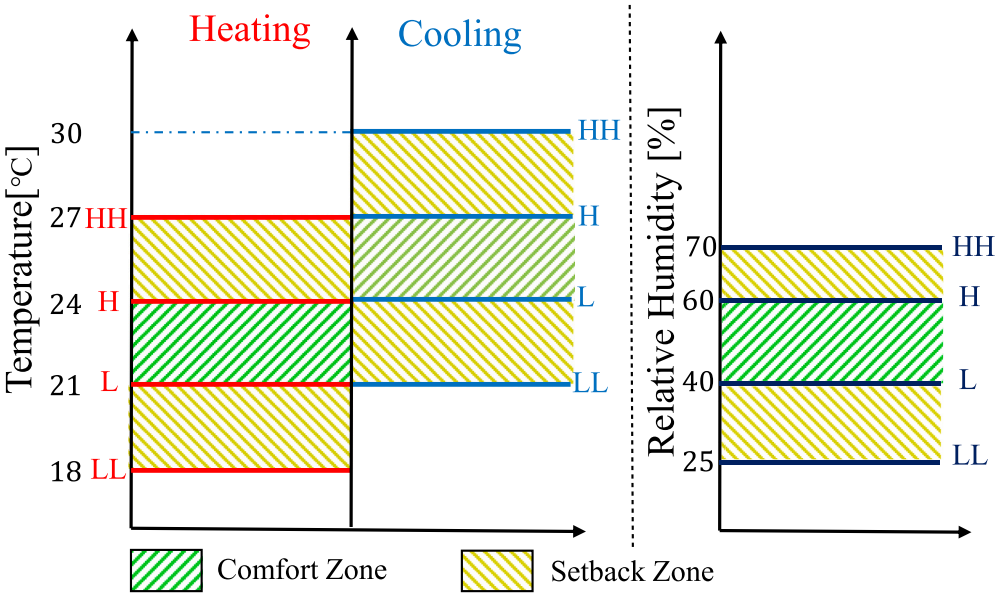

Fig. 2. Illustration of the comfort and setback ranges for indoor temperature and humidity. The figure defines the acceptable ranges for maintaining comfort used to adjust indoor conditions. In this figure, HH, H, L, and LL represent HighHigh, High, Low, and LowLow, respectively [10,41,58,60].

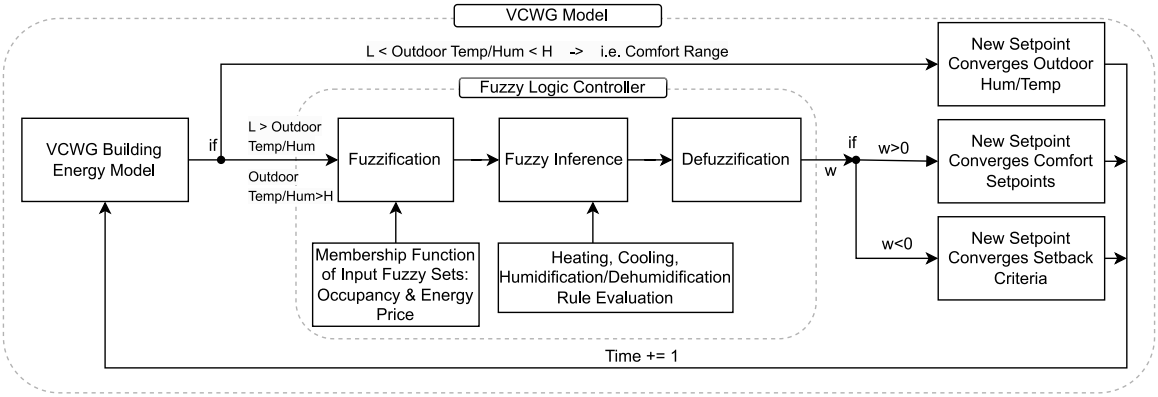

Fig. 3. Flowchart illustrating the integration of the Weather-Adaptive Fuzzy Control (WAFC) with the Vertical City Weather Generator (VCWG v3.0.0) software. The diagram outlines the process of dynamically adjusting temperature and humidity setpoints based on occupancy, energy price, and external conditions.

2.3. Weather-Adaptive Fuzzy Control (WAFC)

This study introduces Weather-Adaptive Fuzzy Control (WAFC), a novel real-time strategy that dynamically adjusts indoor temperature and humidity setpoints to optimize energy efficiency and comfort. This method has been integrated with the VCWG software according to the flowchart in Fig. 3. The core principle of this method is to closely track external conditions and adjust the indoor setpoint accordingly whenever feasible. The VCWG model first calculates the building parameters based on the previous setpoint. If the outdoor temperature/humidity falls within the comfort range, the indoor setpoint converges to the outdoor condition. However, if the outdoor temperature/humidity is outside the comfort range, the FLC controller determines whether the indoor setpoint should converge to the comfort or setback conditions, based on the sign of a control variable w to be positive or negative. The controller, generates new setpoints for temperature and humidity. The approach integrates a fuzzy inference system that evaluates external factors using linguistic variables, enabling adaptive control of indoor conditions for improved energy savings. The comfort ranges are defined in Fig. 2 for humidity and temperature. These ranges are obtained from [10,41,58,60]. It should also be noted that the basic thermostat mode for cooling setpoint is 27 °C and for the heating setpoint is 22 °C.

According to the FLC process diagram illustrated in Fig. 8, which follows Mamdani's Fuzzy Inference System (FIS) [61], the controller employs FLC to determine the w parameter that governs the adaptation of setpoints.

To do so, first, the system uses predefined membership functions to assess the input's degree of membership. The controller uses two fuzzy variables: occupancy level [Person m^{-2}] and time of day [hr]. It is assumed in this study that maximum five

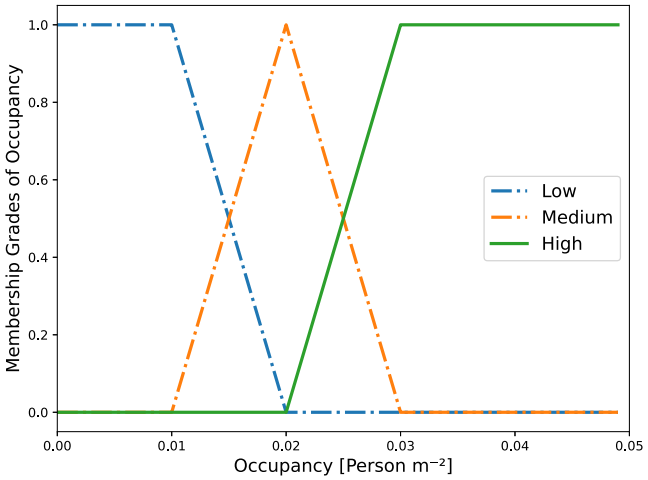

Fig. 4. Fuzzy membership functions for the occupancy variable in the building. The functions are categorized into low, medium, and high occupancy levels, using trapezoidal and triangular shapes to represent varying degrees of occupancy.

Table 2
Time-Of-Use (TOU) electricity pricing scheme.

TOU period	Summer hours	Winter hours
Off-peak	From 7 p.m. to 7 a.m.	From 7 p.m. to 7 a.m.
Mid-peak	From 7 a.m. to 11 a.m., 5 p.m. to 7 p.m.	From 11 a.m. to 5 p.m.
On-peak	From 11 a.m. to 5 p.m.	From 7 a.m. to 11 a.m., 5 p.m. to 7 p.m.

persons are living in a residential-detached house of 100 m^2 with three membership functions as: Low, Medium, and High, using trapezoidal/triangular shapes to capture varying levels of occupant presence (Fig. 4). These membership functions overlap to ensure smooth transitions between categories, avoiding abrupt changes in system behavior. Low occupancy corresponds to sparse presence, where the membership function peaks for values below 0.01 Person m^{-2}. Medium occupancy covers moderate presence, with its membership function peaking between 0.01 and 0.03 Person m^{-2}. High occupancy represents dense presence, with its membership function dominating above 0.03 Person m^{-2} (Fig. 4).

For electricity price we have used the Time-Of-Use (TOU) pricing scheme in Ontario, Canada, as an example reflecting different electricity costs during different periods of the day and season, for which the details can be found in Table 2. It is important to note that the differences in electricity prices between Winter and Summer, as well as between weekdays and weekends, have been accounted for in this study. The electricity price in the fuzzy logic system is represented by three membership functions: Low, Medium, and High, using trapezoidal shapes (Figs. 5 and 6). Low price corresponds to off-peak hours, with the membership function peaking for the lowest electricity rates (Row Number 1 in Table 2). Medium price is associated with mid-peak hours and is represented by a trapezoidal membership function, peaking during medium electricity pricing levels (Row Number 2 in Table 2). High price corresponds to on-peak hours, where the membership function dominates for the highest electricity rates (Row Number 3 in Table 2). In this membership function, the x-axis represents time, and the y-axis represents the degree of membership. For example, in Ontario, during Summer, as shown in Table 2, the medium peak price occurs from 7 a.m. to 11 a.m. and again from 5 p.m. to 7 p.m. Consequently, in the membership function (Fig. 5), these two time periods correspond to the medium degree of membership, while the degrees of membership for low and high prices are zero during these intervals.

Following the fuzzy inference process, we apply the fuzzy rules defined in Table 3 to the fuzzified input variables (electricity price and occupancy level) to determine the output variable w. Factor w which governs HVAC setpoint adjustments, is defined using three triangular membership functions: Negative (N), Zero (Z), and Positive (P). The Negative (N) category corresponds to scenarios where the indoor setpoint converges toward outdoor or setback conditions, prioritizing energy savings. The Positive (P) category represents adjustments toward comfort conditions, ensuring occupant comfort. Zero (Z) indicates no change in the setpoint, maintaining current indoor conditions.

To illustrate the application of the FLC in our study, a brief example of its setpoint control mechanism is provided in the Winter. For the two input variables, occupancy and energy price, two distinct sets of membership functions are defined, as depicted in Fig. 8. These functions assign a membership value to each element of a fuzzy set (Low, Medium, and High) for each physical input, effectively translating numerical data into symbolic representations. For instance, given a scheduled occupancy of 0.01 Person m^{-2} at 10:00 a.m., the corresponding degrees of membership for Occupancy and Electricity Price are (1 Low, 0 Medium, and 0 High) and (0 Low, 1 High, and 0 Medium), respectively.

In this scheme we have different sets of control rules for heating, cooling, humidification, or dehumidification. The rules are outlined in Table 3, which differentiate between weekday and weekend strategies for the Summer and Winter. Specifically, weekend

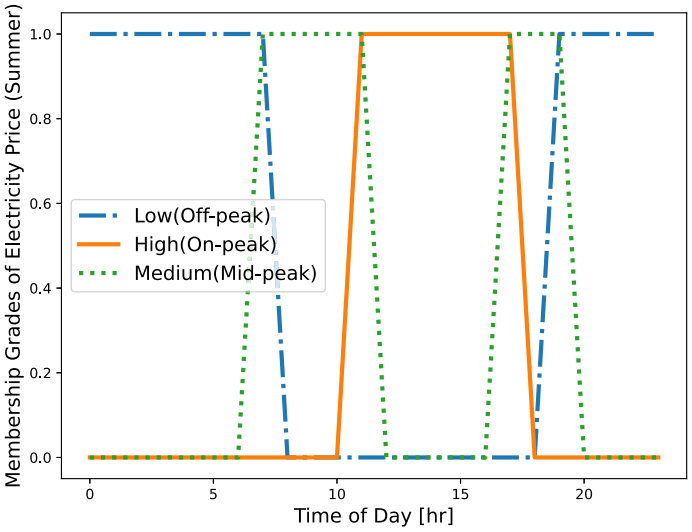

Fig. 5. Fuzzy membership functions for the price variable in Summer, which reflects the cost of electricity. The categories include low, medium, and high price ranges, representing different time-of-use pricing periods throughout the day.

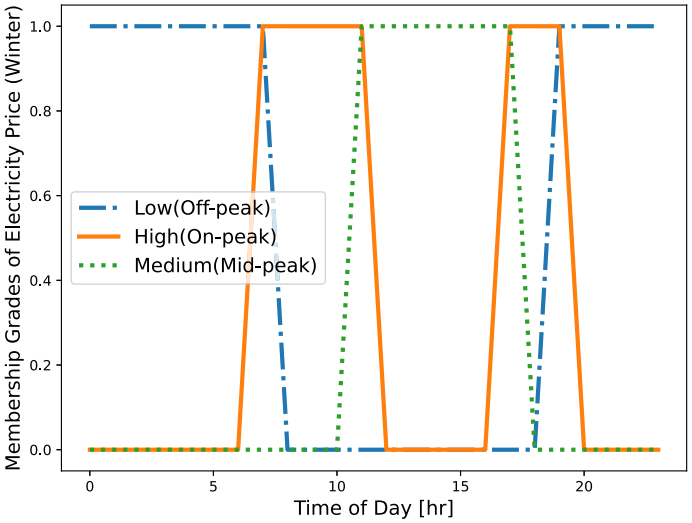

Fig. 6. Fuzzy membership functions for the price variable in Winter, which reflects the cost of electricity. The categories include low, medium, and high price ranges, representing different time-of-use pricing periods throughout the day.

rules do not account for electricity price fluctuations since rates remain constant throughout the day and night. In contrast, heating and humidification rules are not dependent on electricity price fluctuations, as these processes utilize natural gas in the HVAC system. Given that gas prices remain constant throughout the day and night in Canada, gas prices have not been considered a fuzzy input for these processes. Conversely, cooling and dehumidification require a refrigeration cycle, and thus electricity, so the corresponding rules depend on electricity price. In this table N means the setpoints should converge to outdoor conditions, P means the setpoints should converge to comfort levels, and Z means no change.

Regarding Table 3 for cooling during weekdays, when occupancy is low and the electricity price is low, medium, or high, the system should attempt to converge to the outdoor conditions, which is likely higher than the indoor and comfort setpoints. This corresponds to the linguistic variable N in our rule definition. In this scenario, energy efficiency takes precedence over comfort considerations when occupancy is low. Subsequently, when occupancy is medium and the price is low, the system converges to the comfort level P, while a medium price results in no change Z, and a high price increases convergence to the outdoor level N. Finally, high occupancy with low, medium, and high prices prompts convergence to the comfort level P.

Different aggregation methods, such as Min (AND), Max (OR), and Product, can be utilized depending on the specific requirements of a problem. In our application, we have selected the Max (OR) operator to ensure that the system can respond

Table 3
Combined rules for HVAC adjustments based on occupancy presence, electricity price, and day type (weekdays and weekends): N: Converging to outdoor, Z: No change, P: Converging to comfort setpoint.

Function	Day type	Occupancy	Electricity price	w Adjustment
Cooling/Dehumidification	Weekday	Low	Low	N
		Low	Medium	N
		Low	High	N
		Medium	Low	P
		Medium	Medium	Z
		Medium	High	N
		High	Low	P
		High	Medium	P
		High	High	P
	Weekend	Low	–	N
		Medium	–	Z
		High	–	P
Heating/Humidification	All days	Low	–	N
		Medium	–	Z
		High	–	P

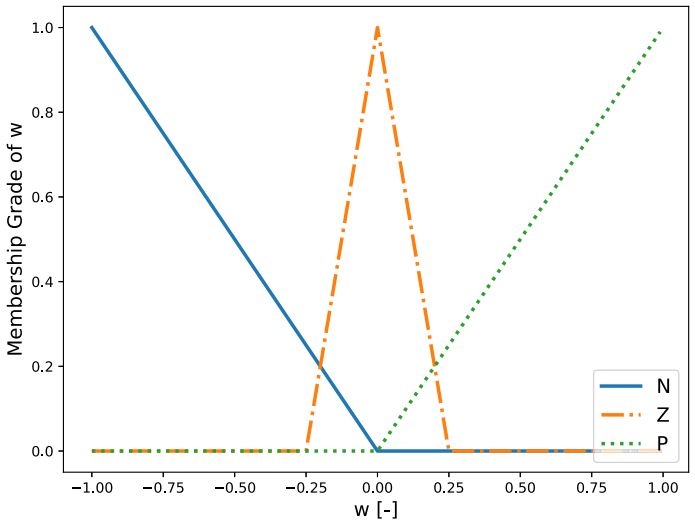

Fig. 7. Fuzzy membership functions for temperature and humidity setpoints' adjustments. Both temperature and humidity adjustments use similar membership functions categorized into Negative (N), Zero (Z), and Positive (P) to guide the control of HVAC system setpoints.

effectively to either high electricity prices or low occupancy levels, whichever is more critical at a given time. This approach provides flexibility and ensures that the temperature and humidity setpoints are adjusted based on the most significant influencing factor. By using the Max (OR) operator, we simplify the decision-making process while maintaining both responsiveness and energy efficiency [62]. In this process, the degree of membership of different fuzzy inputs is used to determine the system's response to those linguistic variables and their respective degrees of membership. With the Max (OR) operation method, the output value for the linguistic variables corresponds directly to the highest activation levels, as shown in the third column of the table presented in Fig. 8. We use the Minimum (Min) implication method, where the output membership function is truncated to the input's degree of membership. This method ensures the system's response is proportional to the input activation and complements the Max aggregation approach for efficient real-time control.

Following the aggregation of the output linguistic variables using the Max (OR) operation method, the next step is the defuzzification process. In this step, the fuzzy outputs obtained earlier are converted into a crisp value (w) that can be utilized to adjust the setpoints.

The fuzzy output membership function employed in this study is a triangular membership function designed to calculate w, which controls the heating, cooling, humidification, or dehumidification setpoints (Fig. 7). It includes three categories: N, Z, and P, ensuring a consistent and adaptable control strategy across all of these processes. The P and N values of these membership functions determine whether the smart setpoint should follow outdoor conditions or adhere to predefined comfort setpoints, dynamically adjusting the setpoints based on real-time input data.

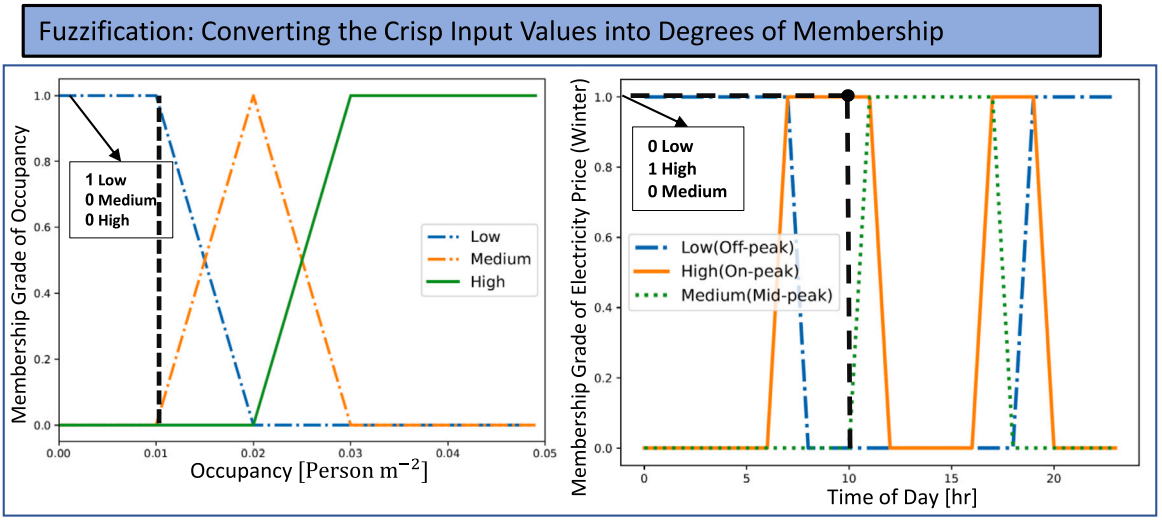

Rule Evaluation and Aggregation: Applying the Fuzzy Rules to the Fuzzified Inputs

Occupancy	Elec. Price	Activation Level	Area Allocated Name
Low (1)	Low (0)	N [max(1,0)=1)]	A1
Low (1)	Medium (0)	N [max(1,0)=1)]	A2
Low (1)	High (1)	N [max(1,1)=1)]	A3
Medium (0)	Low (0)	P [max(0,0)=0)]	A4
Medium (0)	Medium (0)	Z [max(0,0)=0)]	A5
Medium (0)	High (1)	N [max(0,1)=1)]	A6
High (0)	Low (0)	P [max(0,0)=0)]	A7
High (0)	Medium (0)	P [max(0,0)=0)]	A8
High (0)	High (1)	P [max(0,1)=1)]	A9

Min Operation (AND), Max Operation (OR), Product Operation

Fig. 8. This diagram illustrates an example of the process of converting crisp input values into degrees of membership and applying the rule table to calculate the activation levels.

The defuzzification process utilizes the centroid method, also known as the center of gravity or center of area method, to compute a specific numerical output for the w variable. This involves calculating the areas under the membership functions, denoted as A_1 to A_9, corresponding to the output fuzzy sets. The centroid method calculates the center of mass of these fuzzy sets by determining the weighted average of their areas. The formula used is

$$\text{Output} = C = w = \frac{\sum_i (C_i A_i)}{\sum_i A_i} \tag{8}$$

where C_i represents the centroid of the ith fuzzy set, and A_i is the area under the ith fuzzy set. By determining the weighted average of these centroids, the method effectively finds the balance point, yielding a crisp value that influences the final decision on setpoint adjustments to optimize both energy efficiency and occupant comfort.

In this example, using the activation levels in the third column of the table in Fig. 8, the respective allocated areas can be determined, which have been denoted in the fourth column. These areas have been color-coded to reflect the respective area in the next Fig. 9. In this figure, the centroid of the ith fuzzy set has been calculated, and then the centroid method has been used to obtain the center of gravity of all areas. The final value for this example input is $C = w = -0.4$, which is a negative value.

In this context, the negative value of w adjusts the smart setpoint by moving it toward the setback condition (as illustrated in the decision tree in Fig. 3), whereas a positive value of w forces the smart setpoint to converge toward comfort condition.

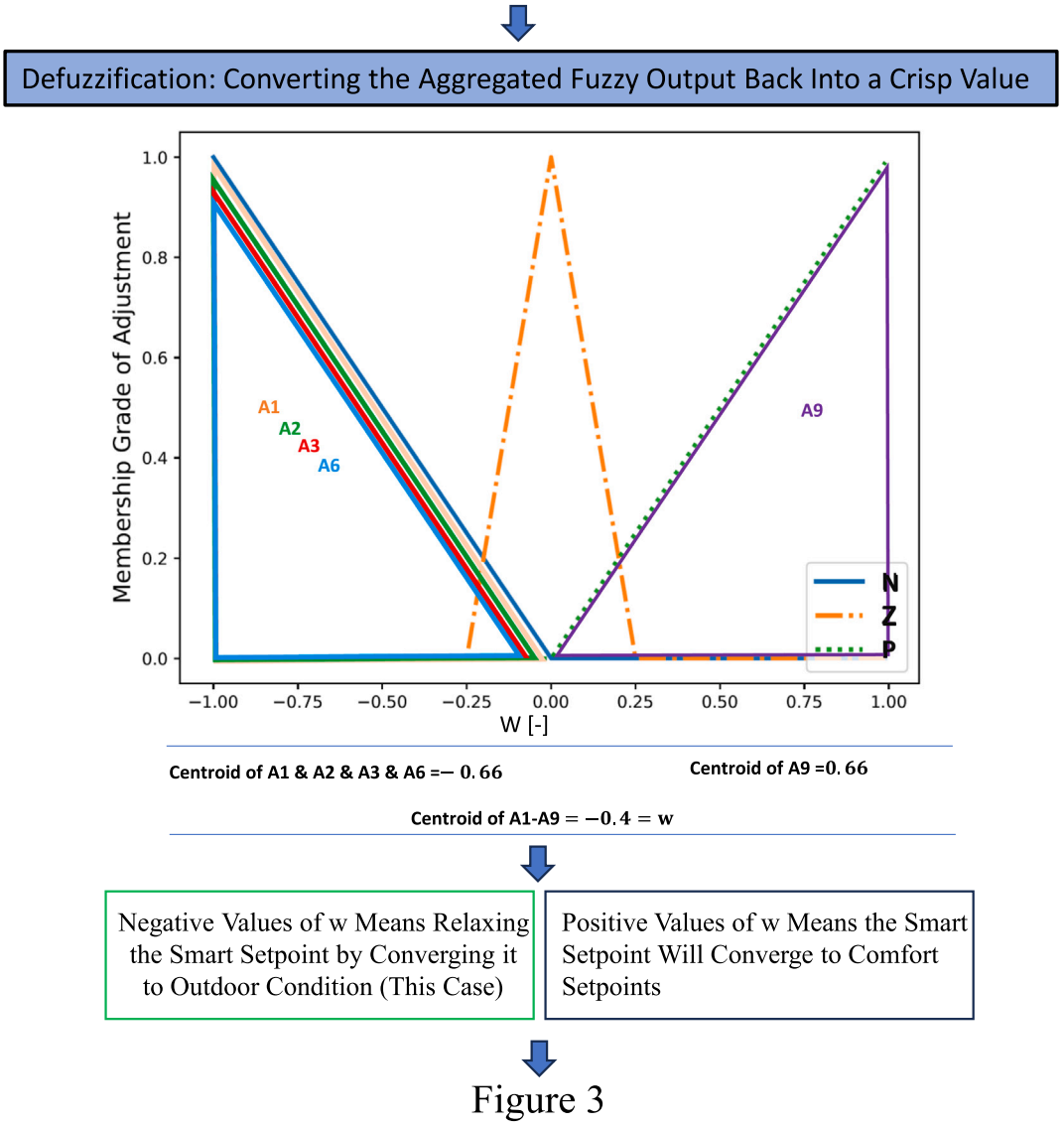

Fig. 9. Diagram representing the color-coded areas for each input. The Centroid method is applied to determine the center of gravity for all areas.

3. Results and discussion

3.1. Performance of the Weather-Adaptive Fuzzy Control (WAFC) in selected months

The model has been run for a whole year. The total runtime for a year is almost half an hour on 1 CPU, which is incredibly fast for a holistic urban physics model. In the following, we present the results for selected months with Air Change per Hour ACH = 1.5 h^{-1} (infiltration) to demonstrate how the model operates. Three months, such as January, representing a cold season, May, representing a shoulder season, and July, representing a warm season, were selected.

In January, during heating mode, the outdoor temperature is predominantly very cold, around 0 °C. Consequently, the indoor temperature alternates between the L setpoint (comfort condition) and the LL setpoint (setback condition). In our model, the occupancy behavior varies throughout the day, peaking at midnight and decreasing during midday (Fig. 10). At time 0 [hr] (midnight), the occupancy is at its maximum. According to the rules specified in Table 3 and the FLC rules, the indoor temperature converges to the comfort setpoint. In Fig. 11(a), we can note four temperature bands (LL, L, H, HH). These bands, as explained earlier, represent the constant comfort and setback setpoints. Additionally, there is a fuzzy-controlled real-time setpoint that continuously aims to create the most energy-efficient setpoint. The indoor temperature consistently converges to this setpoint, aligning with it; therefore, in the subsequent figures, we only display the indoor temperature. Also, in these figures, there are some important time

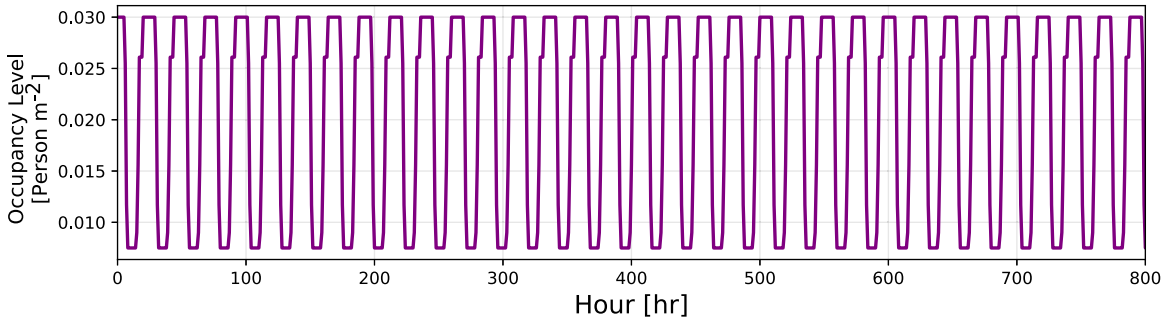

Fig. 10. Variation of occupancy level throughout the month.

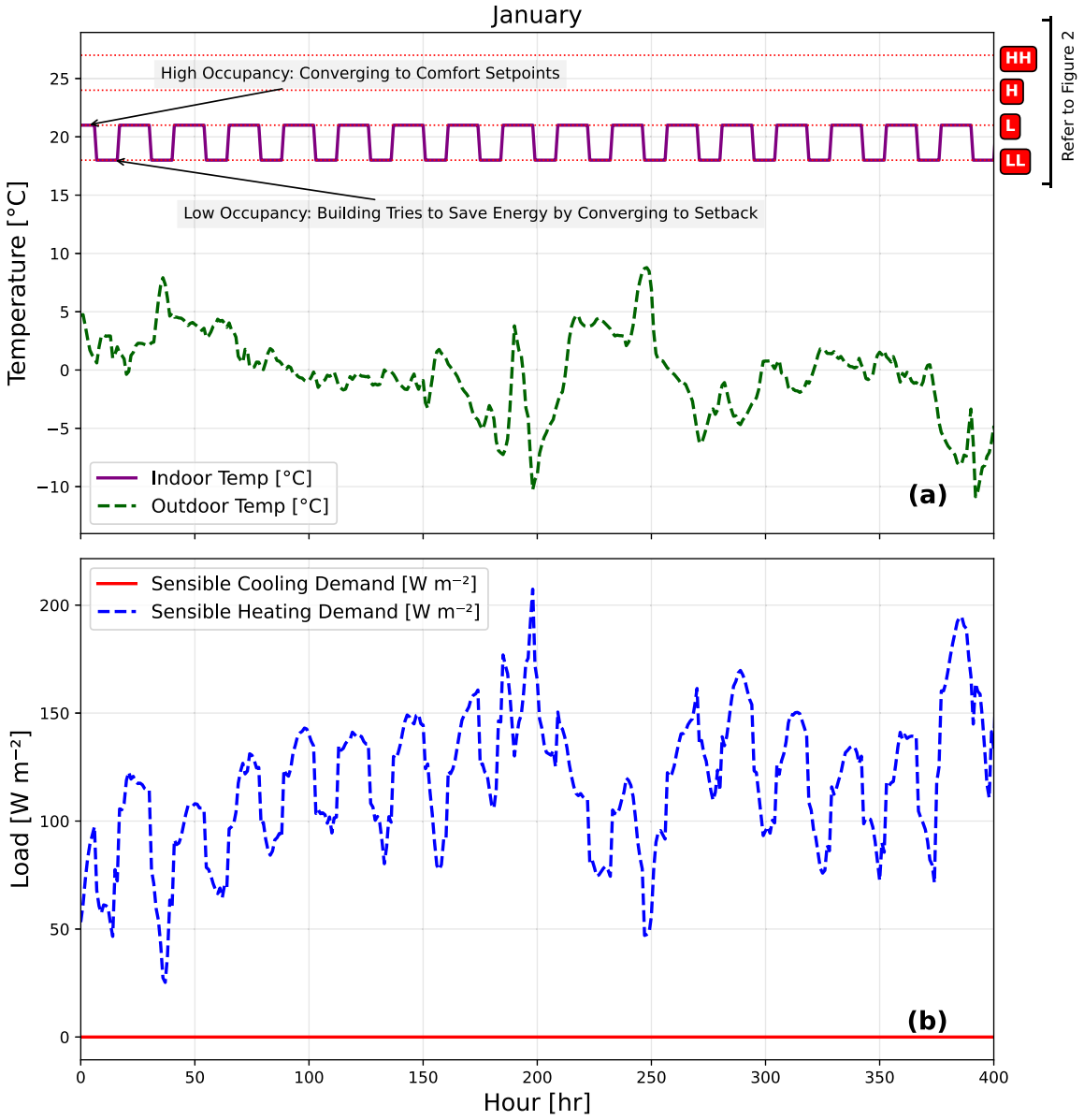

Fig. 11. (a) Indoor temperature variations and (b) sensible heating and cooling load variations, both for January, showing the system's response to occupancy changes, electricity prices, and outdoor conditions.

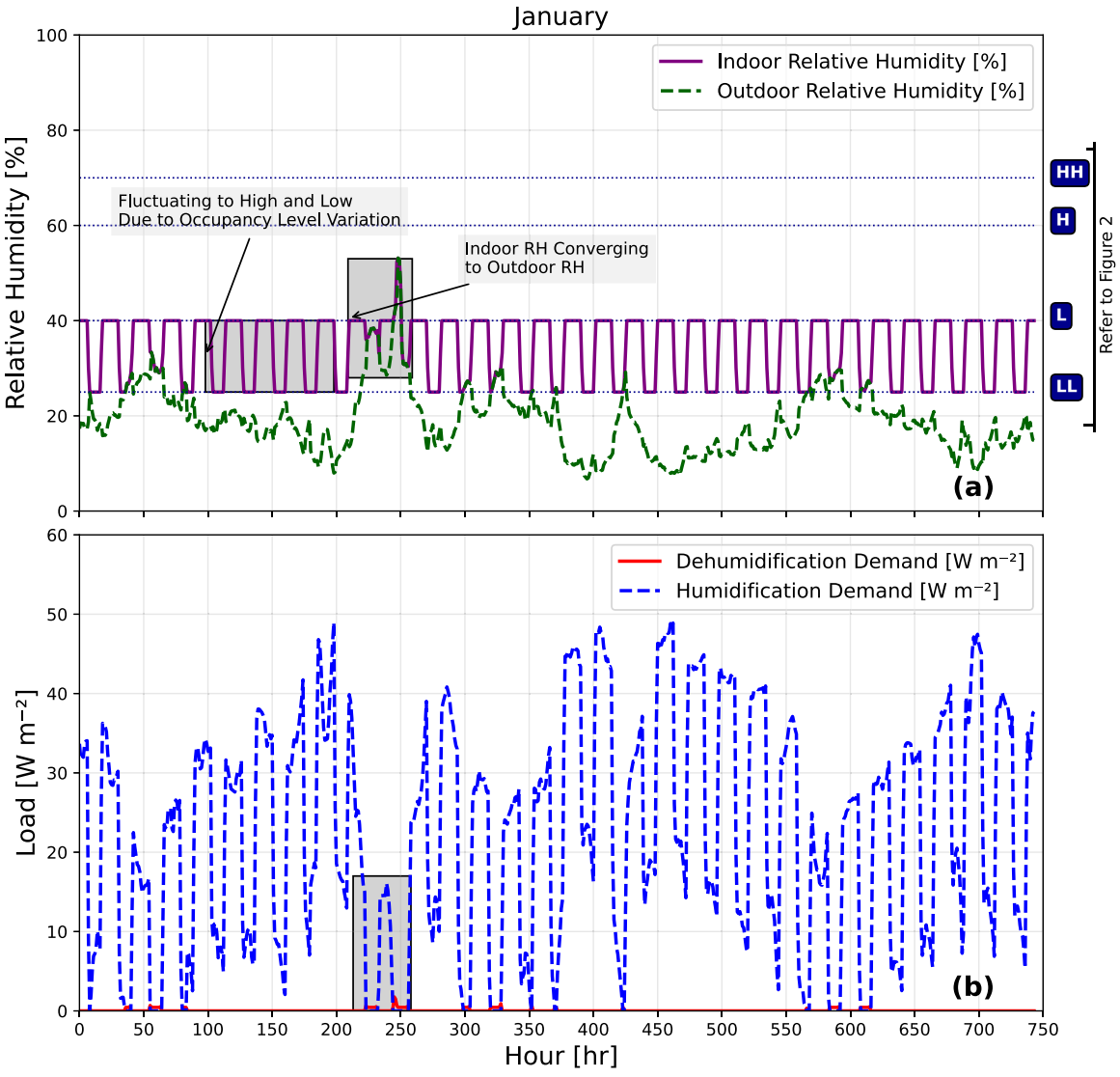

Fig. 12. (a) Indoor RH variations and (b) latent (Humidification/Dehumidification) load variations, both for January, showing the system's response to occupancy changes, electricity prices, and outdoor conditions.

durations that highlight how the system and model work, and they have been annotated in the figures. For January, as can be seen in Fig. 11(b), the cooling sensible demand is zero, and the heating demand varies. As can be seen, when the outdoor temperature dives down, the heating load increases as the temperature difference between the setpoint and outdoor increases.

It is noteworthy that, within the comfort range defined between L and H levels, the system always selects the closest comfort level. For instance, during Winter, when the outdoor temperature is lower than the L level, the system converges to the L level to optimize energy efficiency. As the morning progresses and occupancy decreases while electricity prices increase, the model aims to adjust the indoor temperature closer to the outdoor temperature. However, reducing the temperature to very cold levels (e.g., 0 to 5 °C) is impractical due to pre-heating requirements. Therefore, the indoor temperature is limited to an LL threshold, set at 18 °C. This behavior represents the basic operation of the modeled HVAC system when the outdoor temperature is either higher than HH or lower than LL.

The smart Relative Humidity (RH) control depicted in Fig. 12(a) demonstrates a stable toggling of humidification demand between the L and LL setpoints from 100 to 200 h. It is noteworthy that, during this month, due to the dry outdoor conditions, the building primarily experiences a humidification load. This fluctuation is influenced by occupancy and energy price inputs, as the outdoor humidity remains below the LL threshold. Around 220 h, when the outdoor RH exceeds the LL threshold, the indoor RH gradually converges to the outdoor conditions to save energy. These energy savings are reflected in the latent load calculations shown in Fig. 12(b). The respective range has been highlighted in this figure, illustrating a decline in humidification demand.

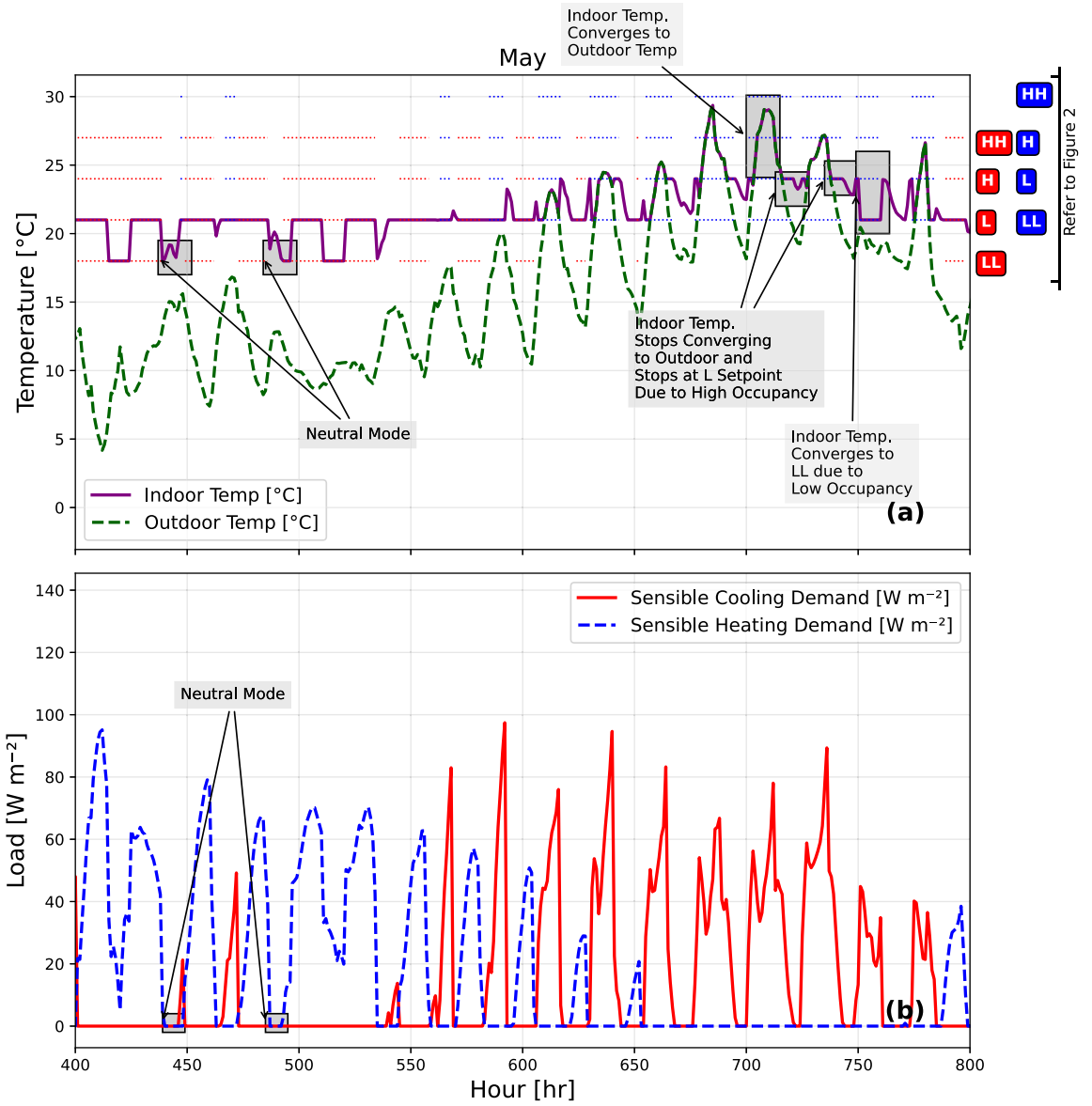

Fig. 13. (a) Indoor temperature variations and (b) sensible heating and cooling load variations, both for May, showing the system's response to occupancy changes, electricity prices, and outdoor conditions.

May is a shoulder season, during which the building experiences heating, cooling, or neutral modes, resulting in a complex response to inputs. Fig. 13(a) illustrates the temperature behavior, while Fig. 13(b) shows the corresponding sensible heating and cooling loads. The right side of Fig. 13(a) displays the four temperature bands, as represented in Fig. 2, marked in blue and red. Analyzing the temperature and load profiles, it is evident that the building is predominantly in heating mode during the first half of the month, which aligns with the blue threshold lines indicating comfort and setback criteria for control, particularly between 400 and 600 h. In the second half of the month, as the outdoor temperature rises, the system occasionally enters a neutral mode, indicated by the absence of red or blue lines, where no sensible heating or cooling is required. This occurs when both sensible load calculations for cooling and heating demand yield negative values (according to Eq. (1)). During these periods, the indoor temperature remains within the comfort zone when occupancy is high, whereas, when occupancy is low, the indoor temperature may fall outside the comfort range.

In May, as the outdoor temperature fluctuates, the system responds by balancing comfort and energy efficiency. Around 700 h, the outdoor temperature rises from the L (blue) setpoint to approximately 28 °C, causing the indoor temperature to converge towards the outdoor temperature within the comfort range (between L and H). To minimize HVAC loads, the system allows the indoor temperature to follow the outdoor condition. As the temperature rises beyond H (blue) to 28 °C, it exceeds the comfort

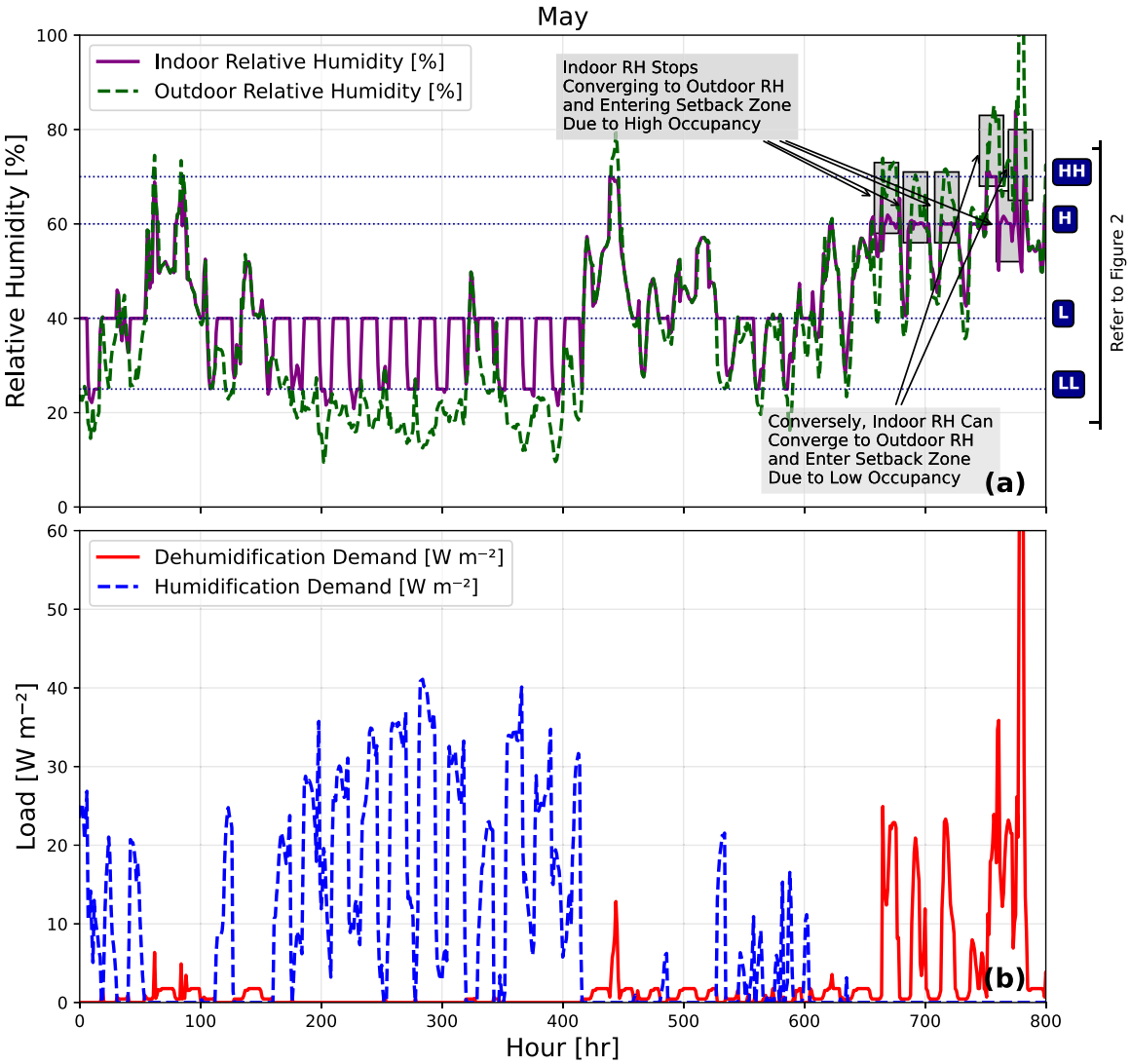

Fig. 14. (a) Indoor RH variations and (b) latent (Humidification/Dehumidification) load variations, both for May, showing the system's response to occupancy changes, electricity prices, and outdoor conditions.

zone. However, since occupancy is low, the indoor temperature is still allowed to converge with the outdoor condition until around 720 h. At this point, when the outdoor temperature drops below L (blue) and occupancy is high, the system maintains the indoor temperature within the comfort level. This cycle repeats around 725 h. After the high occupancy period ends and with the outdoor temperature below the LL (blue) setpoint, the system prioritizes energy savings, allowing the indoor temperature to converge with the outdoor temperature, capped at the LL level.

In May, the smart humidity control system effectively balances energy efficiency and occupant comfort, responding to dynamic humidity conditions. Fig. 14(a) shows the behavior of the smart humidity control, while Fig. 14(b) highlights the presence of both humidification and dehumidification loads throughout the month. During the period between 200 and 300 h, the relative humidity (RH) profile fluctuates between the L and LL levels, representing comfort and setback conditions. These fluctuations are primarily influenced by occupancy and electricity pricing, with outdoor humidity consistently below the LL threshold. Around 420 h, the outdoor RH exceeds both the LL and L levels, prompting the indoor RH to adjust to these levels to conserve energy. As occupancy decreases, the indoor RH follows outdoor conditions more closely, further optimizing energy efficiency. There are also instances, highlighted in Fig. 14(a), where outdoor RH exceeds the comfort level (H), but due to occupancy and price considerations, the indoor RH remains at H to prioritize comfort. Conversely, later occurrences show that when occupancy and price favor energy savings, the indoor RH converges to the outdoor level and stabilizes at HH, illustrating the adaptive nature of the smart control system.

July, being the warmest month, challenges the building's cooling system with significant temperature fluctuations. As shown in Fig. 15(a), the outdoor temperature often exceeds the HH setpoint (day) and drops below the LL setpoint (night). During the

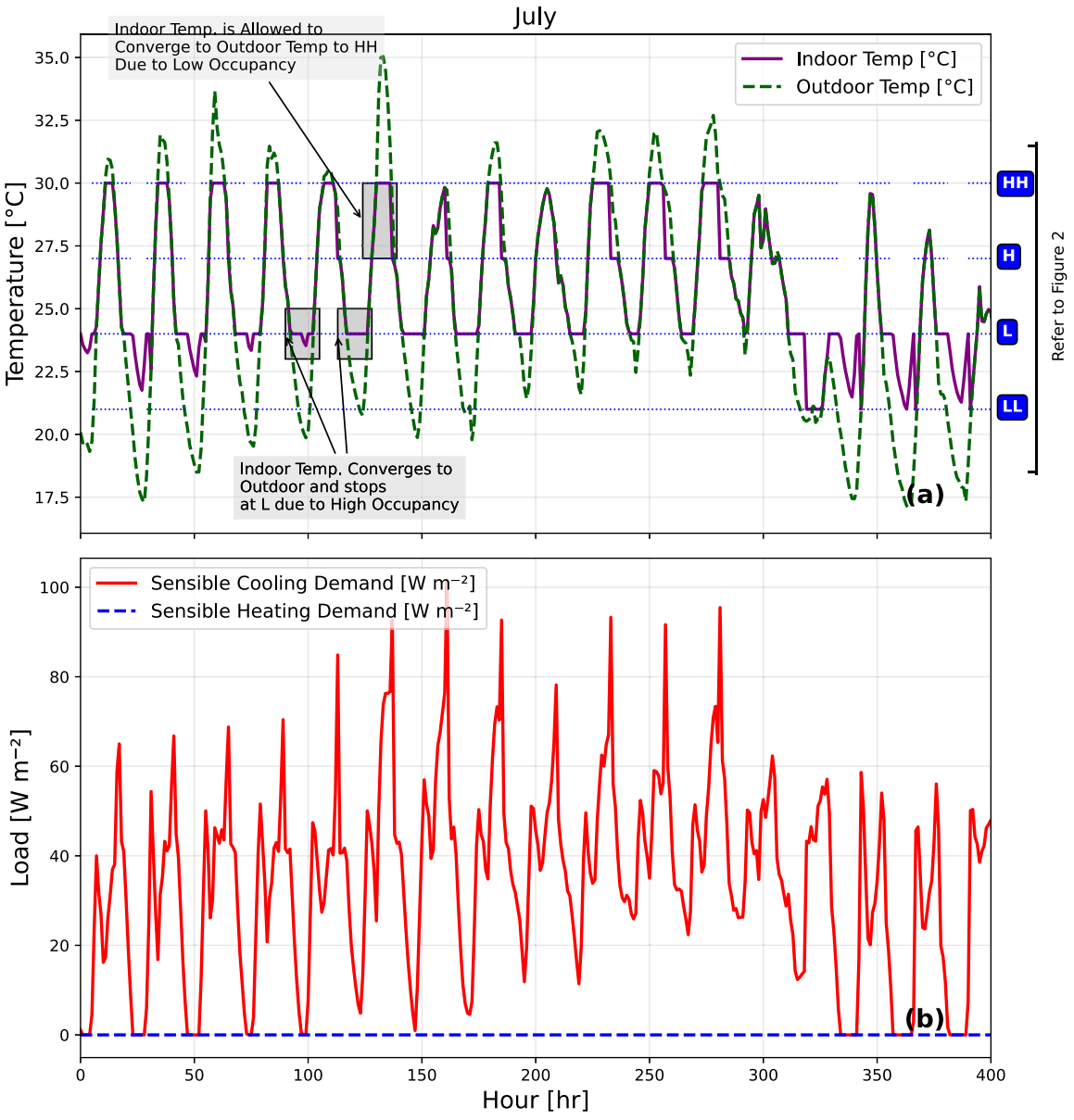

Fig. 15. (a) Indoor temperature variations and (b) sensible heating and cooling load variations, both for July, showing the system's response to occupancy changes, electricity prices, and outdoor conditions.

day, when the outdoor temperatures peak, occupancy is low and energy prices are high, the building setpoint follows the outdoor temperature until it reaches the HH threshold, minimizing sensible cooling loads. At night, when temperatures drop and occupancy is high, the indoor temperature adjusts to the outdoor temperature until it reaches the L level, ensuring thermal comfort. Although energy prices are lower during the night, the FLC prioritizes occupant comfort using the Max operation, adjusting the setpoint accordingly. Consequently, the temperature management strategy emphasizes occupant comfort over cost savings. Overall, as seen in Fig. 15(b), July places the building predominantly in cooling mode due to these high-temperature fluctuations. The variation of the w factor for temperature over time is presented in Fig. 16, for the month of July.

In July, the relative humidity (RH) remains largely within the comfort zone, with indoor RH typically aligning with the target range, as shown in Fig. 17(a). On occasions where outdoor RH is high, the system maintains indoor RH near the H setpoint to ensure comfort. Conversely, during periods of low outdoor RH, particularly near the LL threshold, when occupancy is low and energy prices are high, the system allows the indoor RH to drop to LL to save latent load. These variations in latent load are depicted in Fig. 17(b). The variation of the w factor for humidity over time is presented in Fig. 18, for the month of July.

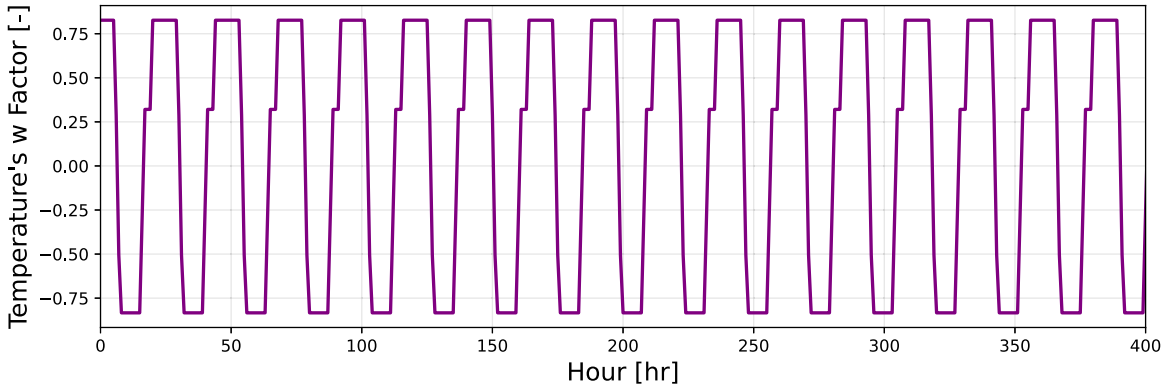

Fig. 16. Variations of the corresponding w factor for temperature across time for the month of July.

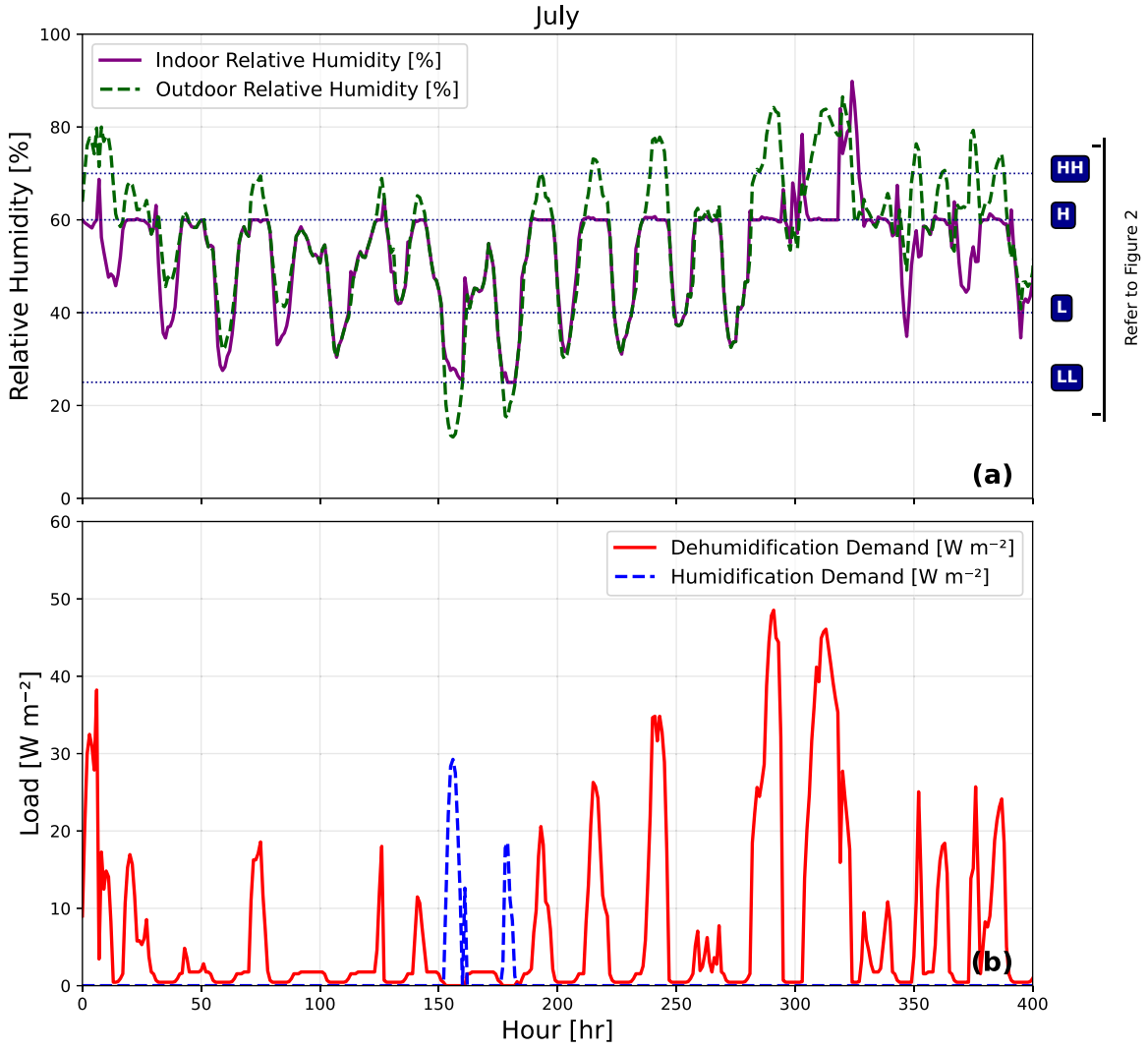

Fig. 17. (a) Indoor RH variations and (b) latent (Humidification/Dehumidification) load variations, both for July, showing the system's response to occupancy changes, electricity prices, and outdoor conditions.

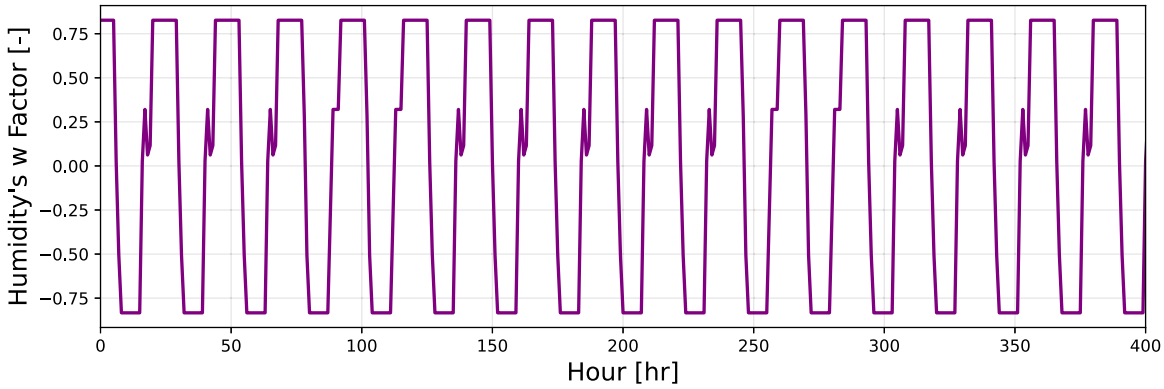

Fig. 18. Variations of the corresponding w factor for humidity across time for the month of July.

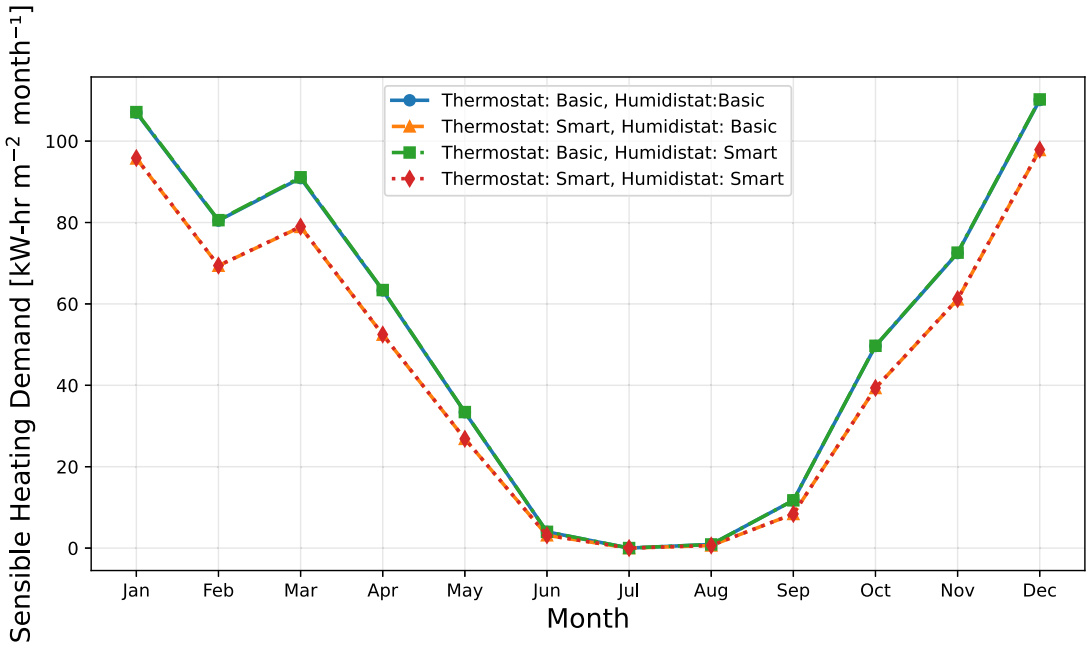

Fig. 19. Comparison of monthly sensible heating demand across four thermostat-humidistat configurations, illustrating the reduction in heating demand achieved with smart setpoint control.

The variation of the w factor for temperature and humidity (Figs. 16 and 18, respectively) illustrate how the fuzzy logic controller adjusts the setpoints dynamically based on the input variables, primarily occupancy levels and electricity price. The results show that the trends for both temperature and humidity w factors closely follow the occupancy patterns, indicating that occupancy has a dominant influence on the system's decision-making process.

3.2. Annual performance given four thermostat-humidistat configurations

The following four figures present a comparative analysis of monthly energy demands across four distinct thermostat-humidistat configurations, highlighting the influence of smart control systems on energy consumption for sensible cooling/heating and latent humidification/dehumidification in various seasonal conditions.

Fig. 19 demonstrates how incorporating smart technology into the thermostat significantly reduces sensible heating demand year-round. Configurations using a smart thermostat, regardless of whether the humidistat is basic or smart, show considerably lower heating demands compared to those using a basic thermostat. This effect is especially pronounced during Winter, when heating requirements peak. The figure reveals that the curves representing the *basic thermostat and basic humidistat* and the *basic thermostat and smart humidistat* configurations are identical, implying that the smart humidistat does not notably influence heating demand when used with a basic thermostat. Likewise, the curves for the *smart thermostat and basic humidistat* and *smart thermostat*

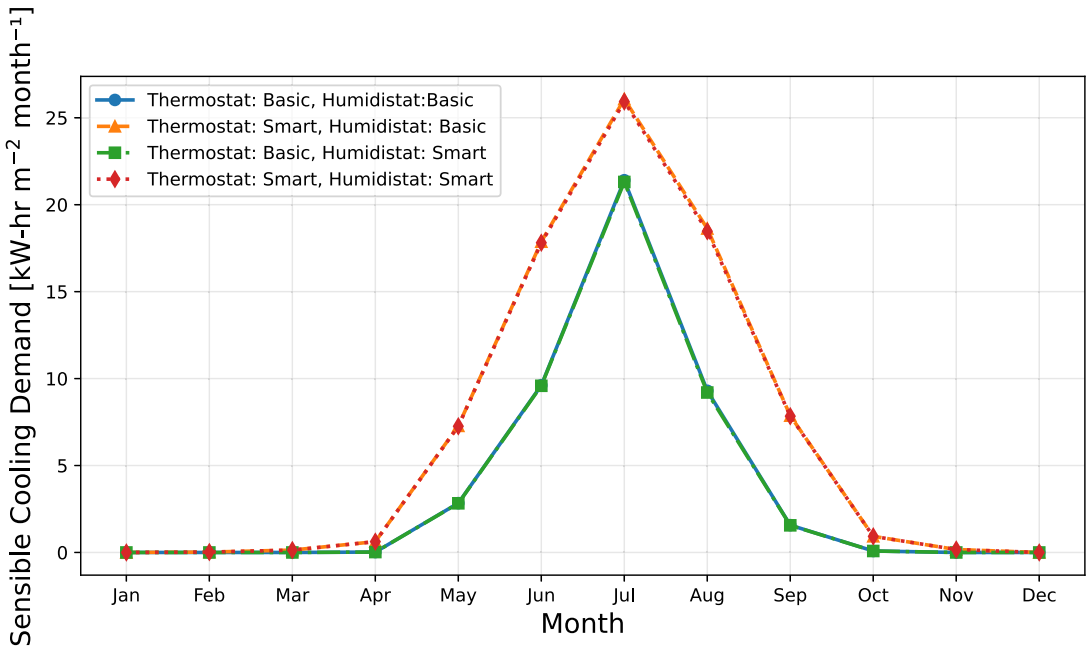

Fig. 20. Sensible cooling demand comparison for various configurations, illustrating increased cooling load with smart setpoint control from May to September and limited impact of the smart humidistat.

Table 4
Energy loads [W-hr m^{-2} month^{-1}] for smart and basic modes in July.

Mode	Infil.	Vent.	Win.	Wall	Ceil.	Mass	Int.	Tran.	Total load
Smart	−854	−303	−427	1 669	2 007	3 285	9 186	11 384	26 147
Basic	−37	−13	−19	631	2 324	1 600	6 772	10 147	21 406

and smart humidistat configurations are also aligned, indicating that the smart humidistat has minimal impact when paired with a smart thermostat.

Fig. 20 illustrates that the use of the smart thermostat results in an increased cooling load, which represents a negative effect observed from May through September. This effect is particularly noteworthy because it contrasts with the expected energy savings associated with smart technologies. The reasons for this behavior are discussed in detail in the following paragraphs. Additionally, the figure shows that the smart humidistat is ineffective in reducing sensible cooling loads, as its influence is limited primarily to latent loads.

Table 4 presents the breakdown of sensible cooling loads for both smart and basic buildings. The summation of all loads is provided in the last column. The summation accounts for the hours when the building is under active cooling mode (i.e., the components of the load under neutral conditions are not accounted for). The table shows the breakdown of the components of load in Fig. 20 for July. The table reveals that the smart system outperforms the basic system in terms of infiltration, ventilation, and window flux loads, as the loads are more negative. However, in terms of conductive heat transfer, through walls and mass, the basic system performs better, resulting in a higher overall cooling load for the smart system.

During the warmer months in Canada, when the system operates in cooling mode (starting in late May, as shown in Fig. 13(a), and lasting until September), the outdoor temperature typically fluctuates between the setpoints. In the smart approach employed in this study, the system attempts to converge indoor temperatures to the outdoor temperature, so the air exchange loads are reduced by minimizing the temperature difference between the setpoint and outdoor temperature. This leads to a reduction in air exchange loads, including infiltration and ventilation. Table 4 confirms that the infiltration and ventilation loads are significantly lower in the smart mode.

However, again referring to Table 4, the use of the smart thermostat also results in a considerable increase in building structure temperatures (wall and mass), which can be attributed to greater temperature fluctuations in the building under smart control. For instance, at midday, when the outdoor temperature is high, the system allows the building to warm up to conserve energy. Later, as the cooling need is required due to high occupancy, the thermal inertia of the building's structure causes a delayed response, resulting in a temperature differential between the structure and the setpoint, thereby increasing the corresponding components of load (wall and mass). This situation is particularly evident during periods of rapid temperature changes. Further, under the smart mode, the number of hours that the building is cooled is greater than in the basic mode. As stated earlier, the components of the

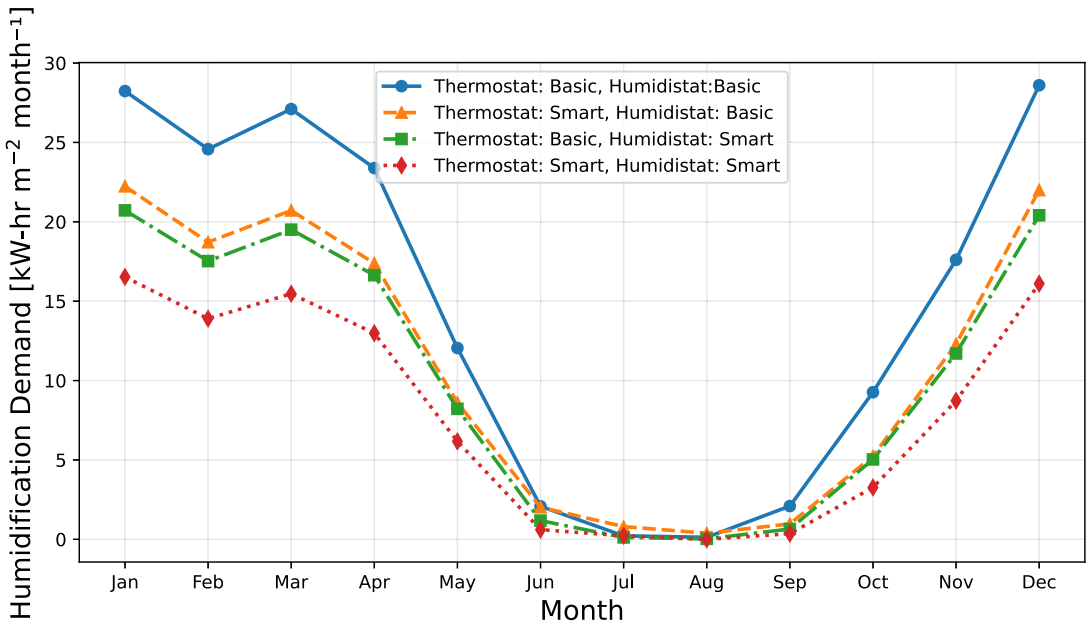

Fig. 21. Humidification demand comparison for various configurations, illustrating decreasing latent load with smart setpoint control, particularly for cold months.

load are only summed under cooling conditions. Therefore, this results in other components of the load being greater for the smart mode, such as the internal load.

Fig. 21 shows that the humidification demand is subject to significant seasonal variation, with the highest demand observed during the colder months, such as January and February. This pattern is consistent with the increased need for humidification in Winter due to lower ambient humidity levels in the climate of Toronto. When cold outdoor air infiltrates indoor spaces and is heated to room temperature, its relative humidity decreases significantly. This dry air can lead to discomfort and health issues, necessitating increased humidification to maintain indoor thermal comfort. In contrast, during the warmer months, such as July and August, the humidification demand is minimal across all configurations, likely due to naturally higher levels of environmental humidity in the climate of Toronto.

Among the four configurations, the combination of a smart thermostat with a smart humidistat demonstrates the most consistent reduction in energy consumption throughout the year. This result highlights the effectiveness of advanced control algorithms in adapting to seasonal and daily fluctuations and maintaining optimal indoor humidity with minimal energy input. By contrast, the combination of a basic thermostat and a basic humidistat consistently shows the highest humidification demand across most months, underscoring the inefficiency of legacy systems that lack dynamic control capabilities.

The intermediate configurations, those with either a smart thermostat paired with a basic humidistat or a basic thermostat paired with a smart humidistat, exhibit performance trends that vary depending on the season. For instance, during months with moderate ambient humidity, such as in the Spring and Fall, these configurations occasionally approach the efficiency of the smart-smart combination, suggesting that even partial system upgrades can yield measurable improvements. However, during peak-demand months like January, these intermediate configurations fail to match the energy efficiency of a fully smart system, reinforcing the cumulative benefits of integrating smart technologies at both control points.

Fig. 22 builds on the findings of the previous analysis of humidification demand by providing a complementary examination of dehumidification demand across the same four configurations of thermostat and humidistat systems. Together, these figures offer a nuanced view of the seasonal dynamics of indoor air quality control and the energy implications of employing different levels of system sophistication.

While the humidification demand was observed to peak during the colder months, reflecting the need to compensate for low ambient humidity, the current figure reveals the opposite pattern for dehumidification demand. Here, the highest energy consumption occurs during the Summer months, particularly in July and August, when elevated ambient humidity levels necessitate active dehumidification. This seasonal inverse relationship between humidification and dehumidification demands underscores the dual challenges faced by HVAC systems in maintaining year-round indoor comfort.

The performance trends observed in the dehumidification figure mirror those seen for humidification. The smart thermostat and smart humidistat combination exhibit a low, but not the lowest, dehumidification demand across all months, demonstrating the robust efficiency of fully intelligent systems in adapting to seasonal variations. This configuration's ability to optimize both heating and cooling processes underscores its suitability for year-round energy savings. Conversely, the basic thermostat and basic

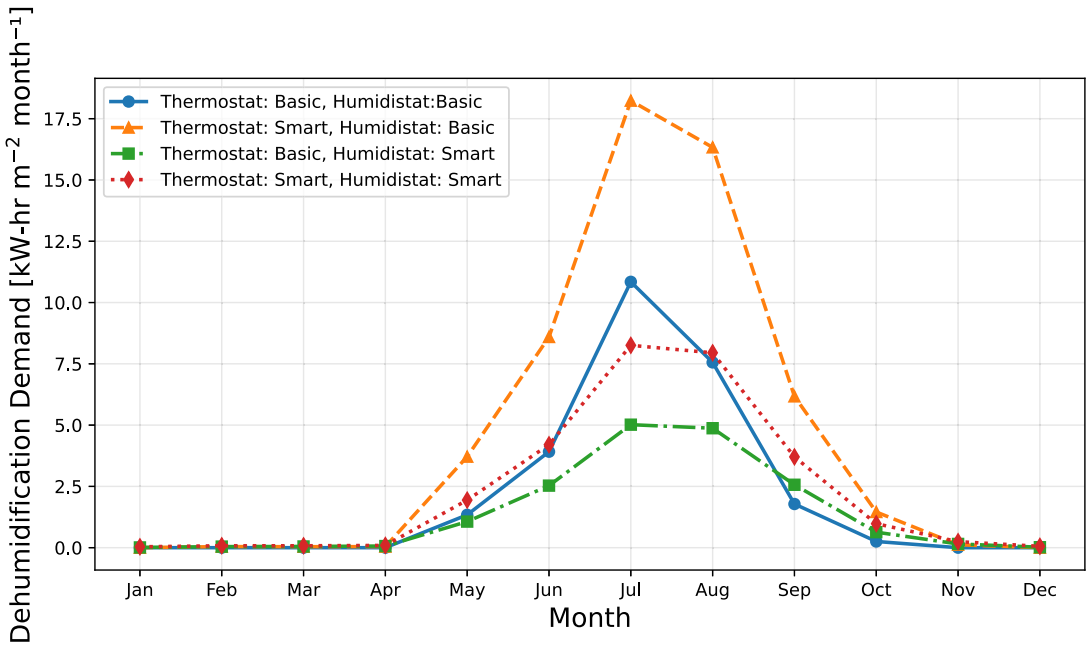

Fig. 22. Dehumidification demand comparison for various configurations, illustrating the nuances in latent load with the utilization of smart setpoint control.

humidistat combination once again show the highest energy demand, indicating inefficiency in managing dehumidification as well as humidification.

By comparing the results across both figures, a clear narrative emerges: smart HVAC systems significantly enhance energy efficiency for both humidification and dehumidification tasks, especially during their respective peak seasons. The complementary nature of these findings highlights the importance of adopting intelligent systems capable of dynamically responding to environmental conditions year-round. The combined evidence strengthens the case for fully integrated smart systems as a critical step toward achieving energy sustainability in climate control technologies.

3.3. Sensitivity to Air Changes per Hour (ACH)

The primary impact of adding smart features to setpoint control lies in the reduction of air exchange loads. Therefore, in this section, the sensitivity of the system to the Air Change per Hour (ACH) rate (infiltration) is analyzed. ACH represents the rate of air leakage in a building, where higher ACH values indicate a leakier building. The data is presented for three air exchange rates: 3, 1.5, and 0.5 h^{-1}. Each bar in the following figures represents the energy savings for a specific month.

Fig. 23, which presents the sensible heating demand, shows that higher ACH results in greater savings. This behavior is consistent across all months and is also evident for humidification, as depicted in Fig. 25. During colder months, infiltration introduces unconditioned air, which is much colder than the comfort temperature, thereby increasing the heating demand. Naturally, as more air enters the building, more unconditioned air needs to be treated. By using smart setpoint control, the system lowers the setpoint as needed to reduce the load. Unlike other smart control designs that require very airtight buildings to be effective, this approach shows promise for older buildings, which typically have higher air leakage rates. This indicates that the leakier the building, the more effective the smart controller becomes.

For cooling, however, there is no consistent trend in energy savings when using smart technologies, as far as different Air Change per Hour (ACH) rates (infiltration) are concerned. As noted earlier, the use of smart control results in increased cooling loads. The reasons for this were discussed in previous sections. Figs. 24 and 26 show the savings in sensible and latent cooling demands for different values of ACH compared to a base case, respectively.

Our results indicate that the total annual energy savings for cooling, heating, dehumidification, and humidification for an air change rate of ACH = 3 h^{-1}, which is based on the ASHRAE standard (Table 1) are −31, 133, −5, and 141 kW-hr m^{-2}, respectively. Although the smart control mode results in an increase in energy demand for cooling and dehumidification, the overall annual performance remains advantageous.

Specifically, when the smart mode is enabled throughout the year, a net energy saving of 238 kW-hr m^{-2} can still be achieved. This positive outcome is primarily due to significant savings in heating and humidification, which outweigh the additional energy costs incurred during cooling and dehumidification. Furthermore, if the smart mode is selectively disabled during the Summer months when it tends to worsen cooling performance, the potential savings increase to 274 kW-hr m^{-2}. In both cases, the control strategy represents a promising opportunity for optimizing energy efficiency without compromising comfort during warmer months.

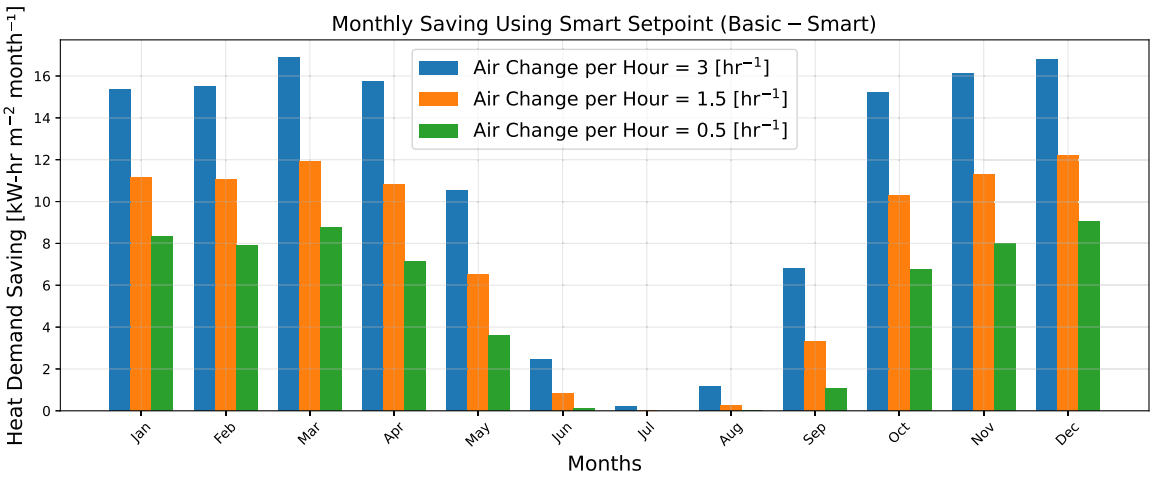

Fig. 23. Sensible Heating demand savings under different Air Change per Hour (ACH) rates. Higher ACH values result in increased energy savings, demonstrating the effectiveness of smart control in reducing heating loads for leaky buildings.

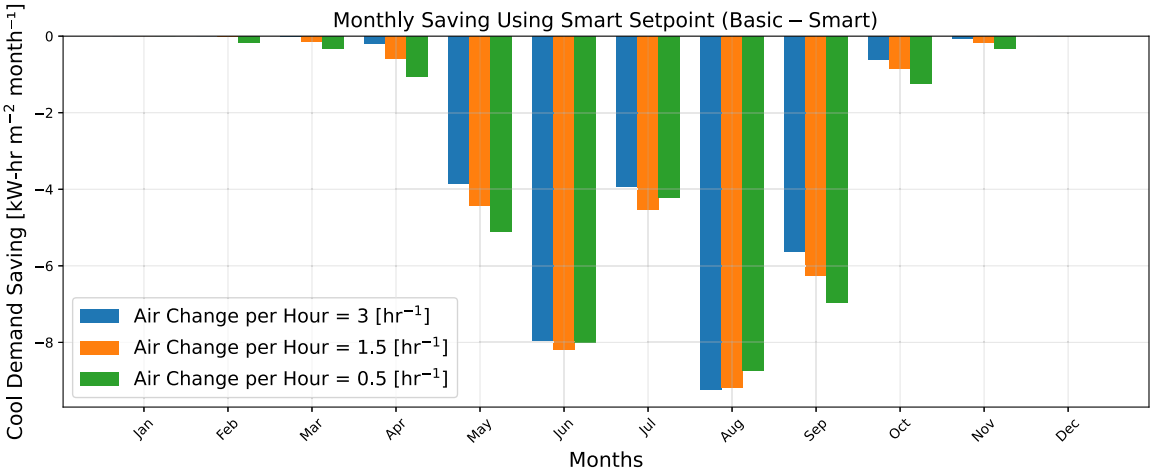

Fig. 24. Sensible cooling demand savings under different Air Change per Hour (ACH) rates.

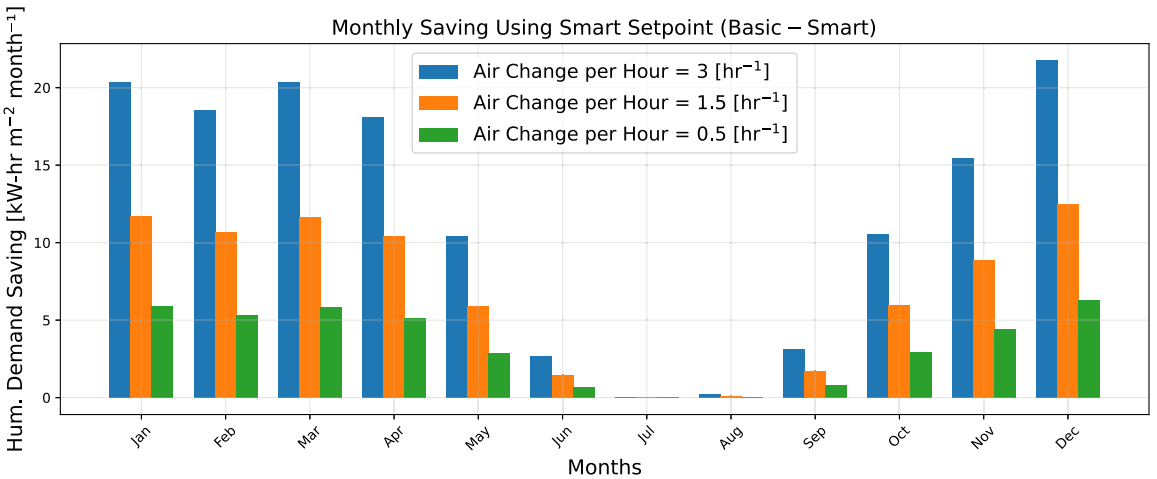

Fig. 25. Humidification demand savings under different Air Change per Hour (ACH) rates. Higher ACH values lead to greater savings, especially during colder months, as smart control adjusts the setpoint to minimize the load.

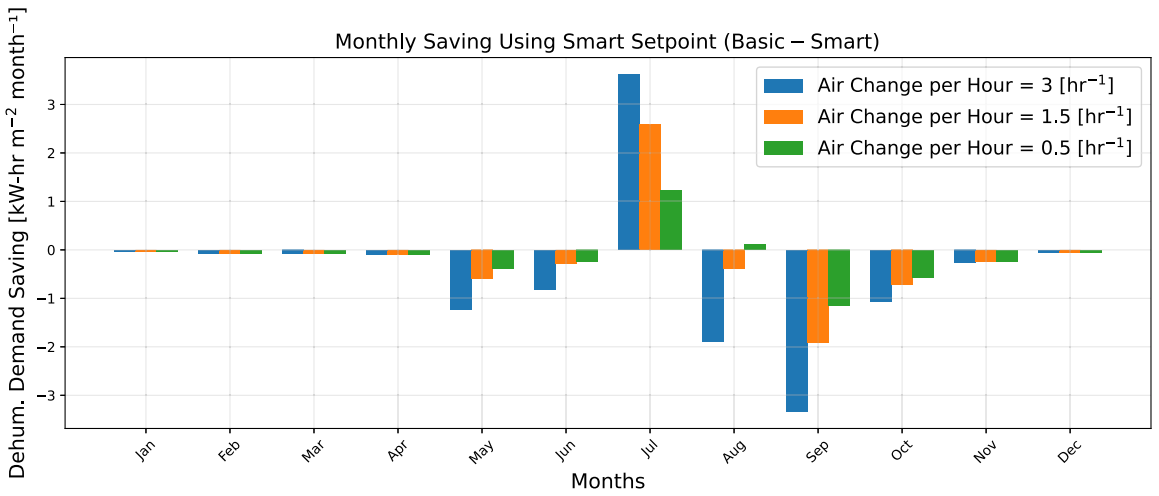

Fig. 26. Dehumidification demand savings under different Air Change per Hour (ACH) rates.

4. Conclusions and recommendations

This study analyzed the impact of smart thermostat and humidistat configurations on building energy efficiency, focusing on heating, cooling, humidification, and dehumidification across different seasonal conditions and air change rates (ACH). The novelty is embedded in considering external weather conditions, electricity prices, and occupancy levels in a fuzzy control framework to adapt indoor setpoints with varying outdoor conditions. We integrated a Fuzzy Logic Control (FLC) scheme into the Vertical City Weather Generator (VCWG v3.0.0) and simulated a detached residential building in the climate of Toronto for a full year in 2020. The results demonstrated both the potential benefits and limitations of employing smart control features to dynamically adjust setpoints based on environmental, occupancy, and energy price inputs.

- The use of smart control showed clear advantages for heating and humidification, underscoring the effectiveness of the Weather-Adaptive Fuzzy Control (WAFC) system in optimizing HVAC operations. The use of smart control showed significant advantages for heating and humidification. During colder months, the smart thermostat effectively reduced heating loads by adjusting setpoints to align with outdoor conditions and occupant requirements, achieving energy savings of up to 133 kW-hr m^{-2}. For humidification, the system saved 141 kW-hr m^{-2} by aligning indoor RH conditions with outdoor RH levels when possible, especially in buildings with high air leakage. These findings confirm the WAFC's ability to optimize HVAC performance in scenarios with high infiltration rates, addressing the challenges associated with older, less airtight buildings.
- Cooling and dehumidification, however, presented challenges. During the warmest months, such as July and August, the smart control mode increased cooling demand by 31 kW-hr m^{-2}, primarily due to temperature fluctuations and higher building structure (wall and mass) loads. Similarly, dehumidification energy demand increased by 5 kW-hr m^{-2}. These results suggest that the smart mode is less effective during the warm season, leading to suboptimal cooling performance. These findings reveal a trade-off in smart control performance during the cooling season, indicating the need to further refine the system to address limitations related to thermal inertia and fluctuating outdoor conditions.
- Despite these challenges, enabling the smart mode throughout the year still resulted in a net energy saving of 238 kW-hr m^{-2}. Moreover, selectively disabling the smart mode during Summer increased potential savings to 274 kW-hr m^{-2}, emphasizing the benefit of a seasonal and flexible control strategy. This approach balances energy efficiency and occupant comfort, suggesting the value of employing smart control features selectively based on seasonal needs.
- Unlike conventional smart control systems, which often require airtight buildings, this strategy shows benefits in existing and leakier buildings by reducing building energy loads due to air exchange. This makes it a practical solution for older buildings with higher air leakage rates. This highlights the WAFC's suitability for retrofitting older buildings, demonstrating its potential for widespread applicability in diverse building types.

In conclusion, while the smart thermostat and humidistat control strategy demonstrated considerable benefits for heating and humidification, they introduced challenges for cooling and dehumidification. A hybrid control strategy, applying smart features only during optimal seasons, could maximize energy savings and minimize drawbacks. Such adaptability makes the control strategy a promising solution for enhancing energy efficiency across a variety of building types, contributing to more sustainable energy management in HVAC systems.

Future investigations could explore the potential for energy savings using this technology in different climate zones. Future work may also involve developing the FLC to work with predictions of outdoor temperature and humidity. For example: (1) a

probabilistic model that utilizes historical hourly weather data to represent each variable (e.g., temperature, humidity) as a normal distribution. By sampling values from these distributions, the model generates realistic predictions of outdoor conditions that account for historical trends and uncertainties. This probabilistic approach provides the system with near-future weather estimates, effectively serving as a predictive control mechanism for dynamic HVAC optimization [63]; (2) a Markov Chain model, where the hourly sequence of past weather conditions in the last few days can provide a near term forecast of outdoor weather conditions. This approach requires a long dataset of past weather over multiple decades to provide reliable probabilities for occurrence of future weather conditions [64,65]; (3) actual weather forecasting using numerical weather prediction models such as the Weather Research and Forecasting (WRF) model [66]; and (4) Model Predictive Control (MPC), where the near-future weather conditions are predicted using a dynamic/mathematical model [27,67].

CRediT authorship contribution statement

Mojtaba Safdari: Writing – review & editing, Writing – original draft, Software, Methodology, Investigation, Data curation, Conceptualization. **Mohammad Al Janaideh:** Writing – review & editing, Supervision. **Kamran Siddiqui:** Writing – review & editing, Writing – original draft, Supervision, Funding acquisition. **Amir A. Aliabadi:** Writing – review & editing, Writing – original draft, Visualization, Validation, Supervision, Software, Methodology, Investigation, Funding acquisition, Formal analysis, Data curation.

Declaration of Generative AI and AI-assisted technologies in the writing process

During the preparation of this work, the author(s) used GPT-4-turbo in order to correct for grammar and spelling of the text. After using this tool/service, the author(s) reviewed and edited the content as needed and take(s) full responsibility for the content of the publication.

Declaration of competing interest

The authors declare that they have no known competing financial interests or personal relationships that could have appeared to influence the work reported in this paper.

Acknowledgments

This work was supported by the University of Guelph through the International Doctoral Tuition Scholarship (IDTS); the Discovery Grant program (401231) from the Natural Sciences and Engineering Research Council (NSERC) of Canada; and the Climate Action and Awareness Fund (CAAF) (055725) from Environment and Climate Change Canada (ECCC).

Availability of code and data

The Atmospheric Innovations Research (AIR) Laboratory at the University of Guelph provides the model source code. For access, contact Amir A. Aliabadi (aaliabad@uoguelph.ca), visit http://www.aaa-scientists.com/, or visit https://github.com/AmirAAliabadi.

Data availability

The Atmospheric Innovations Research (AIR) Laboratory at the University of Guelph provides the model source code. For access, contact Amir A. Aliabadi (aaliabad@uoguelph.ca), visit http://www.aaa-scientists.com/, or visit https://github.com/AmirAAliabadi.

References

[1] A. Madadizadeh, K. Siddiqui, A.A. Aliabadi, Review: The economics landscape for building decarbonization, Sustain. 16 (14) (2024) 6214, http://dx.doi.org/10.3390/su16146214.
[2] International Energy Agency, World Energy Outlook 2023, International Energy Agency, Paris, 2023, URL: https://www.iea.org/reports/world-energy-outlook-2023.
[3] W. Miller, B. Sodagar, D. Whaley, K. Bamdad, S. Zedan, Mind the gap: A comparison of socio-technical limitations of national house rating systems in the UK and Australia, J. Build. Eng. 43 (2021) 102570, http://dx.doi.org/10.1016/j.jobe.2021.102570.
[4] H. Chaouch, C. Çeken, S. Arı, Energy management of HVAC systems in smart buildings by using fuzzy logic and M2M communication, J. Build. Eng. 44 (2021) 102606, http://dx.doi.org/10.1016/j.jobe.2021.102606.
[5] I. Asadi, N. Mahyuddin, P. Shafigh, A review on indoor environmental quality (IEQ) and energy consumption in building based on occupant behavior, Facilities 35 (11/12) (2017) 684–695.
[6] N. Aqilah, H.B. Rijal, S.A. Zaki, A review of thermal comfort in residential buildings: Comfort threads and energy saving potential, Energies 15 (23) (2022) 9012.
[7] H. Chen, S. Liu, M. Eftekhari, Y. Li, W. Ji, Y. Shen, Experimental studies on the energy performance of a novel wavy-shape Trombe wall, J. Build. Eng. 61 (2022) 105242, http://dx.doi.org/10.1016/j.jobe.2022.105242.
[8] X. Zhang, I. Reda, M. Aram, D. Qi, L.L. Wang, H. Fellouah, Wind-driven smoke dispersion in rooftop photovoltaic fires: An experimental investigation with helium smoke, J. Build. Eng. 83 (2024) 108467, http://dx.doi.org/10.1016/j.jobe.2024.108467.
[9] P.O. Fanger, Thermal Comfort: Analysis and Applications in Environmental Engineering, Danish Technical Press, Allinge, 1970.

[10] ASHRAE, ASHRAE Handbook - Fundamentals, Technical Report, American Society for Heating Refrigeration and Airconditioning Engineers, Peachtree Corners, 2021.
[11] M. Esrafilian-Najafabadi, F. Haghighat, Occupancy-based HVAC control systems in buildings: A state-of-the-art review, Build. Environ. 197 (2021) 107810.
[12] W. Tushar, T. Wang, L. Lan, Y. Xu, C. Withanage, C. Yuen, K.L. Wood, Policy design for controlling set-point temperature of ACs in shared spaces of buildings, Energy Build. 134 (2017) 105–114.
[13] V. Fabi, R.V. Andersen, S.P. Corgnati, Influence of occupant's heating set-point preferences on indoor environmental quality and heating demand in residential buildings, HVAC R Res. 19 (5) (2013) 635–645.
[14] R. Yang, M.W. Newman, Learning from a learning thermostat: lessons for intelligent systems for the home, in: F. Mattern, S. Santini, J.F. Canny, M. Langheinrich, J. Rekimoto (Eds.), Proceedings of the 2013 ACM International Joint Conference on Pervasive and Ubiquitous Computing, Association for Computing Machinery, New York, 2013, pp. 93–102.
[15] D.W.U. Perera, C.F. Pfeiffer, N.-O. Skeie, Control of temperature and energy consumption in buildings: a review, Int. J. Energy Environ. 5 (4) (2014) 471–484.
[16] D.S. Naidu, C.G. Rieger, Advanced control strategies for heating, ventilation, air-conditioning, and refrigeration systems—An overview: Part I: Hard control, HVAC R Res. 17 (1) (2011) 2–21.
[17] J. Širokỳ, F. Oldewurtel, J. Cigler, S. Prívara, Experimental analysis of model predictive control for an energy efficient building heating system, Appl. Energy 88 (9) (2011) 3079–3087.
[18] S. Taheri, P. Hosseini, A. Razban, Model predictive control of heating, ventilation, and air conditioning (HVAC) systems: A state-of-the-art review, J. Build. Eng. 60 (2022) 105067, http://dx.doi.org/10.1016/j.jobe.2022.105067.
[19] X. Xin, Z. Zhang, Y. Zhou, Y. Liu, D. Wang, S. Nan, A comprehensive review of predictive control strategies in heating, ventilation, and air-conditioning (HVAC): Model-free VS model, J. Build. Eng. 94 (2024) 110013, http://dx.doi.org/10.1016/j.jobe.2024.110013.
[20] A. Keshtkar, S. Arzanpour, F. Keshtkar, An autonomous system via fuzzy logic for residential peak load management in smart grids, in: 2015 North American Power Symposium, NAPS, IEEE, Piscataway, 2015, pp. 1–6.
[21] A. Beheshtikhoo, M. Pourgholi, I. Khazaee, Design of type-2 fuzzy logic controller in a smart home energy management system with a combination of renewable energy and an electric vehicle, J. Build. Eng. 68 (2023) 106097, http://dx.doi.org/10.1016/j.jobe.2023.106097.
[22] H. Zhang, L. Wang, W. Shi, Seismic control of adaptive variable stiffness intelligent structures using fuzzy control strategy combined with LSTM, J. Build. Eng. 78 (2023) 107549.
[23] F. Behrooz, N. Mariun, M.H. Marhaban, M.A. Mohd Radzi, A.R. Ramli, Review of control techniques for HVAC systems—Nonlinearity approaches based on fuzzy cognitive maps, Energies 11 (3) (2018) 495.
[24] M.K. Farimani, S. Karimian-Aliabadi, R. Entezari-Maleki, B. Egger, L. Sousa, Deadline-aware task offloading in vehicular networks using deep reinforcement learning, Expert Syst. Appl. 249 (2024) 123622.
[25] H. Mirinejad, S.H. Sadati, M. Ghasemian, H. Torab, Control techniques in heating, ventilating and air conditioning systems, J. Comput. Sci. 4 (9) (2008) 777.
[26] Y. Song, S. Wu, Y.Y. Yan, Control strategies for indoor environment quality and energy efficiency—a review, Int. J. Low-Carbon Technol. 10 (3) (2015) 305–312.
[27] A. Afram, F. Janabi-Sharifi, Theory and applications of HVAC control systems–A review of model predictive control (MPC), Build. Environ. 72 (2014) 343–355.
[28] M. Farrokhifar, H. Bahmani, B. Faridpak, A. Safari, D. Pozo, M. Aiello, Model predictive control for demand side management in buildings: A survey, Sustain. Cities Soc. 75 (2021) 103381.
[29] M. Xu, S. Li, Practical generalized predictive control with decentralized identification approach to HVAC systems, Energy Convers. Manage. 48 (1) (2007) 292–299.
[30] H. Khajeh, H. Laaksonen, M.G. Simões, A fuzzy logic control of a smart home with energy storage providing active and reactive power flexibility services, Electr. Power Syst. Res. 216 (2023) 109067.
[31] M. Woźniak, J. Szczotka, A. Sikora, A. Zielonka, Fuzzy logic type-2 intelligent moisture control system, Expert Syst. Appl. 238 (2024) 121581.
[32] M. Hamdi, G. Lachiver, A fuzzy control system based on the human sensation of thermal comfort, in: 1998 IEEE International Conference on Fuzzy Systems Proceedings. IEEE World Congress on Computational Intelligence (Cat. No.98CH36228), Vol. 1, Piscataway, 1998, pp. 487–492, http://dx.doi.org/10.1109/FUZZY.1998.687534.
[33] J.J. Aguilera, O.B. Kazanci, J. Toftum, Thermal adaptation in occupant-driven HVAC control, J. Build. Eng. 25 (2019) 100846, http://dx.doi.org/10.1016/j.jobe.2019.100846.
[34] M. Ardehali, M. Saboori, M. Teshnelab, Numerical simulation and analysis of fuzzy PID and PSD control methodologies as dynamic energy efficiency measures, Energy Convers. Manage. 45 (13–14) (2004) 1981–1992.
[35] T.F. Megahed, S.M. Abdelkader, A. Zakaria, Energy management in zero-energy building using neural network predictive control, IEEE Internet Things J. 6 (3) (2019) 5336–5344.
[36] G. Fraisse, J. Virgone, J. Roux, Thermal control of a discontinuously occupied building using a classical and a fuzzy logic approach, Energy Build. 26 (3) (1997) 303–316.
[37] D. Kolokotsa, D. Tsiavos, G. Stavrakakis, K. Kalaitzakis, E. Antonidakis, Advanced fuzzy logic controllers design and evaluation for buildings' occupants thermal–visual comfort and indoor air quality satisfaction, Energy Build. 33 (6) (2001) 531–543.
[38] R.J.P. Barte, T.O. Querimit, J.F. Villaverde, Automatic temperature and humidity control system for tarantula terrarium using fuzzy logic algorithm, in: 2023 15th International Conference on Computer and Automation Engineering, ICCAE, IEEE, Piscataway, 2023, pp. 463–468.
[39] J. Shao, Z. Zhong, X. Xu, Investigation on weights setting rule for weights-based fuzzy logic control algorithm utilized in direct expansion air-conditioning systems, Int. J. Refrig. 138 (2022) 71–83.
[40] Y. Zhang, Z. Wu, M. Zhang, J. Mai, L. Jin, F. Wang, Smart indoor humidity and condensation control in the spring in hot-humid areas, Build. Environ. 135 (2018) 42–52.
[41] ASHRAE, Standard 62.1: Ventilation and Acceptable Indoor Air Quality, Technical Report, American Society for Heating Refrigeration and Airconditioning Engineers, Peachtree Corners, 2022.
[42] U.E. Habiba, I. Ahmed, M. Asif, H.H. Alhelou, M. Khalid, A review on enhancing energy efficiency and adaptability through system integration for smart buildings, J. Build. Eng. 89 (2024) 109354, http://dx.doi.org/10.1016/j.jobe.2024.109354.
[43] B. Su, S. Wang, An agent-based distributed real-time optimal control strategy for building HVAC systems for applications in the context of future IoT-based smart sensor networks, Appl. Energy 274 (2020) 115322.
[44] A. Capozzoli, M.S. Piscitelli, A. Gorrino, I. Ballarini, V. Corrado, Data analytics for occupancy pattern learning to reduce the energy consumption of HVAC systems in office buildings, Sustain. Cities Soc. 35 (2017) 191–208.
[45] A.A. Aliabadi, Turbulence: A Fundamental Approach for Scientists and Engineers, Springer, Cham, 2022, http://dx.doi.org/10.1007/978-3-030-95411-6.
[46] A.A. Aliabadi, M. Moradi, R.M. McLeod, D. Calder, R. Dernovsek, How much building renewable energy is enough? The vertical city weather generator (VCWG v1.4.4), Atmosphere 12 (7) (2021) 882, http://dx.doi.org/10.3390/atmos12070882.

[47] M. Moradi, B. Dyer, A. Nazem, M.K. Nambiar, M.R. Nahian, B. Bueno, C. Mackey, S. Vasanthakumar, N. Nazarian, E.S. Krayenhoff, L.K. Norford, A.A. Aliabadi, The vertical city weather generator (VCWG v1.3.2), Geosci. Model. Dev. 14 (2) (2021) 961–984, http://dx.doi.org/10.5194/gmd-14-961-2021.
[48] M. Moradi, The Vertical City Weather Generator (Ph.D. thesis), University of Guelph, Guelph, 2021.
[49] M. Moradi, E.S. Krayenhoff, A.A. Aliabadi, A comprehensive indoor–outdoor urban climate model with hydrology: The Vertical City Weather Generator (VCWG v2.0.0), Build. Environ. 207 (2022) 108406, http://dx.doi.org/10.1016/j.buildenv.2021.108406.
[50] A.A. Aliabadi, X. Chen, J. Yang, A. Madadizadeh, K. Siddiqui, Retrofit optimization of building systems for future climates using an urban physics model, Build. Environ. 243 (2023) 110655, http://dx.doi.org/10.1016/j.buildenv.2023.110655.
[51] M. Safdari, R. Ahmadi, S. Sadeghzadeh, Numerical and experimental investigation on electric vehicles battery thermal management under new European driving cycle, Appl. Energy 315 (2022) 119026.
[52] A.A. Aliabadi, R.M. McLeod, The vatic weather file generator (VWFG v1.0.0), J. Build. Eng. 67 (2023) 105966, http://dx.doi.org/10.1016/j.jobe.2023.105966.
[53] M. Safdari, K. Dennis, B. Gharabaghi, K. Siddiqui, A.A. Aliabadi, Implications of latent and sensible building energy loads using natural ventilation, J. Build. Eng. 96 (2024) 110447, http://dx.doi.org/10.1016/j.jobe.2024.110447.
[54] NRCan, National Energy Use Database, Technical Report, Office of Energy Efficiency, Natural Resources Canada, Gatineau, 2020.
[55] USCensusBureau, American Community Survey (ACS), Technical Report, United States Census Bureau, Washington, 2020.
[56] NRCan, National Energy Code of Canada, Technical Report, Office of Energy Efficiency, Natural Resources Canada, Gatineau, 2017.
[57] ASHRAE, Standard 62.2: Ventilation and Acceptable Indoor Air Quality in Residential Buildings, Technical Report, American Society for Heating Refrigeration and Airconditioning Engineers, Peachtree Corners, 2022.
[58] ASHRAE, Standard 90.1: Energy Standard for Buildings Except Low-Rise Residential Buildings, Technical Report, American Society for Heating Refrigeration and Airconditioning Engineers, Peachtree Corners, 2013.
[59] ASHRAE, Standard 90.2: Energy-Efficient Design of Low-Rise Residential Buildings, Technical Report, American Society for Heating Refrigeration and Airconditioning Engineers, Peachtree Corners, 2018.
[60] R. Peters, G. Dubose, R. Maglievaz, R. Cih, Damp Buildings, Human Health, and HVAC Design: Report of the ASHRAE Multidisciplinary Task Group - Damp Buildings, Representing ASHRAE TC 1.12, Moisture Management in Buildings, Technical Report, American Society of Heating, Refrigerating and Air-Conditioning Engineers (ASHRAE), Peachtree Corners, 2020, pp. 1–40, Report of the ASHRAE Multidisciplinary Task Group.
[61] E.H. Mamdani, Application of fuzzy algorithms for control of simple dynamic plant, in: Proceedings of the Institution of Electrical Engineers, Vol. 121, Institution of Engineering and Technology (IET), London, 1974, pp. 1585–1588.
[62] W.W. Tan, T.W. Chua, Uncertain rule-based fuzzy logic systems: introduction and new directions (Mendel, J.M.; 2001) [book review], IEEE Comput. Intell. Mag. 2 (1) (2007) 72–73.
[63] M. Aslani, A. Imanloozadeh, H. Hashemi-Dezaki, M.A. Hejazi, M. Nazififard, A. Ketabi, Optimal probabilistic reliability-oriented planning of islanded microgrids considering hydrogen-based storage systems, hydrogen vehicles, and electric vehicles under various climatic conditions, J. Power Sources 525 (2022) 231100, http://dx.doi.org/10.1016/j.jpowsour.2022.231100.
[64] D. Khiatani, U. Ghose, Weather forecasting using hidden Markov model, in: 2017 International Conference on Computing and Communication Technologies for Smart Nation, IC3TSN, IEEE, Piscataway, 2017, pp. 220–225.
[65] S. Madhwani, C.S. Mansuri, N. Nagarur, Weather forecasting using machine learning and Markov chains, in: IISE Annual Conference. Proceedings, Institute of Industrial and Systems Engineers (IISE), Montreal, 2024, pp. 1–5.
[66] L.E. Ortiz, J.E. Gonzalez, E. Gutierrez, M. Arend, Forecasting building energy demands with a coupled weather-building energy model in a dense urban environment, J. Sol. Energy Eng. 139 (1) (2017) 011002.
[67] S. Huang, Y. Lin, V. Chinde, X. Ma, J. Lian, Simulation-based performance evaluation of model predictive control for building energy systems, Appl. Energy 281 (2021) 116027.